0-9076

Department of Physics

Queen's University
Kingston, Canada

Characterisation of Three Dimensional Fast Ion Electrolytes using Nuclear Mangetic Resonance

D. Amm. M. Sayer and S.L. Segel
Department of Physics, Queen's University

DSS File # 20SU.23440-0-9076

March 1982

REQ. NO. 0-9076

CONTRACT REPORT NO. OSU80-00303

Characterisation of Three Dimensional Fast Ion Electrolytes using Nuclear Magnetic Resonance

DSS File # 20SU.23440-0-9076

D.Amm, M.Sayer and S.L.Segel

Department of Physics

Queen's University

FINAL REPORT

March 1982

Submitted to: Dr. T.A.Wheat

CANMET, Ottawa

59 pp

INDEX

PERSONNEL

ABSTRACT

1. INTRODUCTION

1.1 Nuclear magnetic resonance 3

1.2 NMR in solids 5

1.3 NMR in polycrystalline materials 8

1.4 NMR and ionic conductivity 13

2. EXPERIMENTAL

2.1 NMR spectrometer 14

2.2 Conductivity 15

2.3 Materials preparation 16

2.4 Sample preparation 17

3. RESULTS

3.1 Na β- β " aluminas 18

3.2 Nazirpsios 19

3.3 NYS 26

3.4 NGS 27

4. DISCUSSION

4.1 Diagnostics using nmr 28

4.2 NMR in Nazirpsios 29

5. CONCLUSIONS 34

PERSONNEL

Principal Investigators

S.L.Segel	Professor of Physics Queen's University
M.Sayer	Professor of Physics Queen's University

Graduate Students

D.Amm	Queen's University
D.S.Smith	Queen's University

Consultants

R.J.C.Brown	Department of Chemistry Queen's University
M.F.Bell	Department of Physics Queen's University

Sample preparation was also carried out at McMaster University under the direction of Dr.P.S.Nicholson.

ABSTRACT

The use of nuclear magnetic resonance in the evaluation of the properties of sodium fast ion electrolytes has been reviewed. The ^{23}Na nuclear magnetic resonance of sodium conducting solid electrolytes $Na_{1+x}Zr_2P_{3-x}Si_xO_{12}$ (Nazirpsios) from x=1.8 to x=2.3, $Na_4YSi_4O_{12}$ (NYS) and $Na_5GdSi_4O_{12}$ (NGS) has been investigated in order to establish a correlation between NMR and ionic conductivity in polycrystalline ceramics.

The Nazirpsio ^{23}Na resonances are broad second order quadrupolar resonances with no structure and a width of approximately 15 gauss FWHM at 23 MHz and room temperature. A magnetic field and temperature study of the Nazirpsio resonances shows that narrowing occurs at about 100 C and the narrowed resonance at about 150 C to 200 C is no longer quadrupole coupled. Activation energies for the line narrowing ranged from 0.35 eV to 0.40 eV for x=1.8 to 0.20 eV for x=2.3. The disappearence of the quadrupole coupling is explained by assuming the linewidth is the sum of quadrupole and lifetime (T_1) broadening contributions. In the high temperature region the resonance width is due mostly to lifetime effects and the linewidth activation energy is the same as that of the ion-lattice correlation function. Using an appropriate criterion, attempt-to escape frequencies for ionic hopping can be determined from the nmr data, and reasonable agreement is obtained between electrical conductivity and the nmr data. This indicates that thelattice correlation function for nmr is

almost completely dependent on the ionic diffusion process.

The room temperature sodium resonance in NYS was 30 gauss FWHM with some structure and in NGS, the resonance was about 50 gauss FWHM with no structure. Although the shapes of the sodium resonances changed slightly in the temperature range of 25 C to 250 C, no quantitative information could be extracted and NMR appears to be of limited use for these materials in which only a fraction of the sodium ions are mobile.

Nmr appears to provide rapid characterisation of differences between materials in the β-alumina systems and has interesting theoretical implications in systems where an appreciable fraction of the Na is mobile and isotropic theories are applicable. No clear theory for the nmr resonance applicable to all systems has been established and the interpretation for each material is unique. The use of nmr in the development of proton conductors has been shown to be very valuable, and experimental results obtained during the course of the work suggest a method for automated conductivity testing of production ceramic using the imbalance of an rf bridge.

1. INTRODUCTION:

The abundance of applications for ionic conducting solids has motivated research into solid electrolytes for more than half a century. Some of the potential uses for these materials are in ion concentration measurement devices, electrolysis of water, high temperature heating elements and fuel cells (Hagenmuller and Van Gool, 1978, Wheat, 1981). There is a particularly strong interest in sodium conducting solid electrolytes such as β-β"Alumina and $Na_{1+x}Zr_2P_{3-x}Si_xO_{12}$ (Nazirpsio system) for their application to thermoelectric generators and high energy density batteries. The factors affecting the performance of these materials include the mechanical strength, corrosion resistance and the conductivity. The standard method for the determination of the conductivity is by direct a.c. or d.c. techniques. It is possible, however, to gain information about the ionic conductivity indirectly by using nuclear magnetic resonance (NMR).

1.1 Nuclear Magnetic Resonance

The energy (or Hamiltonian) $\mathcal{H}$ of a magnetic dipole placed in a magnetic field H is given by

$$\mathcal{H} = -\mu \cdot H \qquad (1)$$

Associated with every non-zero nuclear spin I, there is a magnetic dipole moment such that

$$\mathcal{H} = -\gamma h \vec{I} \qquad (2)$$

here γ is called the gyromagnetic ratio. If the magnetic field is taken to be H_0 lying in the z-direction

$$\mathcal{H} = -\gamma \hbar H_0 I_z \qquad (3)$$

and the energy eigenvalues are

$$E = -\gamma \hbar H m \quad \text{where} \quad m = I, I-1, \ldots\ldots, -I$$

and the allowed transitions are between states of $\Delta m = \pm 1$. This gives a transition energy

$$E = \gamma \hbar H = \hbar \omega_L \qquad (4)$$

corresponding to transition frequency $\omega_L = 2\pi\nu_L$.

In the presence of electromagnetic radiation of angular frequency ω_L, the transition probabilities for absorption and stimulated emission are equal, but the Boltzmann factor (exp-E/kT) ensures that the lower energy state is more heavily populated than the higher state, and a net absorption of energy will occur. However, to continue such absorption indefinitely mechanisms must be present to de-excite the higher states. These mechanisms lie in the interaction between the nuclear spins and the surroundings - which for a solid implies the neighbouring lattice atoms. The rate of transfer of energy from the spin system to the lattice is characterised by the longitudinal relaxation time T_1, the time it takes for the spin system to achieve thermal equilibrium. A second type of interaction, related to the decay of components of magnetisation perpendicular to the applied field, and commonly resulting from dipolar interactions between spins, is described by a relaxation time T_2. In the particular case of dipolar effects, the linewidth is inversely proportional to T_2 .

1.2 Nuclear magnetic resonance in solids

Equation (3) gives the frequency at which an isolated spin will absorb power when placed in a magnetic field H. In a solid material, interactions between nuclei and their surroundings may shift the resonance frequency to other values, will cause the resonance to extend over a range of frequencies, and may give rise to a characteristic 'shape' for the resonance in a given crystal structure. A simple interpretation of this is that the surroundings contribute an internal field $H_{lattice}$ in addition to the external field H_o. Since this interaction will be a tensor, in single crystals the form of the resonance will depend upon the orientation of the crystal to the magnetic field, while in polycrystalline samples, the results will be averaged over all possible directions.

In metals, the resonance is shifted by the interaction with the free electron gas (the Knight Shift). However, in ionic solids, only the nucleus-nucleus interaction and the interaction with the fixed lattice must be considered.

(a) Dipolar coupling

The solid is constituted of an array of dipole moments, each of which gives rise to a local magnetic field of approximately μ / r^3. To a first approximation, the Hamiltonian for the energy of the i'th nucleus surrounded by j other nuclei is

$$\mathcal{H} = \gamma_i \hbar \bar{I}_i \left\{ H_o + \sum_{ij}' \frac{\gamma_j \hbar \bar{I}_j}{r_{ij}^3} \right\} \qquad (5)$$

where the sum is over all j nuclei which interact with the i'th nucleus. This creates different magnetic fields at different nuclei and this spread gives a width to the resonance. It can be shown (Abragam 1961) that this width is inversely proportional to the relaxation time T_2 for dipolar coupling. It maybe noted that the linewidth results from a distribution of magnetic fields which essentially remains fixed over a long period of time. If, however, due to motion either of the nucleus or the surroundings, fluctuations occur in the distribution such that the deviations from the mean become small, the nucleus again finds itself in a well-defined field and the linewidth becomes small. This is of importance in the case of solids in which ions are mobile.

(b) Quadrupolar coupling

Quadrupolar coupling results from the interaction of a non-spherical nucleus with an electric field gradient (efg). The interaction term is the product of the quadrupole moment and the efg. Since both of these are tensors, this becomes

$$\mathcal{H}_Q = \frac{1}{6} \sum_{\alpha\beta} V_{\alpha\beta} \, Q_{\alpha\beta} \qquad (6)$$

where α and β run through the x,y, and z directions, V is the efg tensor and Q is the quadrupole moment tensor. In the principal axis frame of the efg, the efg tensor can be described by just two parameters

$$eq = V_{zz} \qquad (7) \qquad\qquad \eta = \frac{V_{xx} - V_{yy}}{V_{zz}} \qquad (8)$$

where V_{zz} is the maximum efg and η is called the asymmetry parameter. e is the electronic charge. By transforming the Hamiltonian to a frame where the magnetic field H_o is along the z-axis and for the special case of $\eta = 0$, the quadrupolar Hamiltonian is written as (Abragam 1961),

$$\mathcal{H}_Q = \frac{3\pi}{40}\left(\frac{e^2 q Q}{I(2I-1)h}\right) f(I,\theta) \qquad (9)$$

where $f(I,\theta)$ is a function of the angle between the magentic field and the maximum efg. If the $\mathcal{H}_Q$ is small compared to the Zeeman term (eqn.3), then $\mathcal{H}_Q$ can be treated as a perturbation to the basic resonance and the resultant energy levels are given by

$$E = E(0) + E(1) + E(2) \qquad (10)$$

where

$$E(0) = -h\,\nu_L\, m$$

$$E(1) = 1/4\; h\,\nu_Q\,(3\cos^2 - 1)(m^2 - 1/3\,a)$$

$$E(2) = h\,\frac{\nu_Q^2}{\nu_L}\, m\left[3/2\,\cos^2\,\sin^2\,(8m^2 - 4a + 1) + 3/8\,\sin^4\,(-2m^2 + 2a - 1)\right]$$

In these expressions, m gives the quantum numbers of the levels involved ($\Delta m = \pm 1$), E(0) gives the frequency of the unperturbed resonance, while E(1) and E(2) gives the effects due to first and second order quadrupolar coupling. The frequencies involved are the following

$$\nu_Q = \frac{3\,e^2 q Q}{h\;2I(2I+1)} \quad ; \quad a = I(I+1) \quad ; \quad \nu_L = \frac{H_o}{2\pi} \qquad (11)$$

It may be noted that E(0) varies directly with H(as in eqn.4), the first order coupling is independent of field, while the second order quadrupolar coupling is inversely proportional to H.

1.3 NMR in polycrystalline materials

The quadrupolar terms introduce a dependence on angle and on the values of m for the initial and final states. In a single crystal the frequency of the resonance will change with rotation within the magnetic field. In the case of polycrystalline samples, the crystallites are distributed randomly over all angles and an average must be taken to determine the NMR 'powder pattern' lineshape.Figure 1.1 shows the results of powder averages for the case of I=3/2 and η =0.The dashed curves are for single crystal lineshapes which are unbroadened, while the solid lines are for crystals showing a finite linewidth due to dipolar interactions. The first order shifts are shown in Figure 1.1(a). The -1/2 ->+1/2 transition is unaffected in first order and these transitions make up the large central peak. The satellite peaks at $\pm\nu_Q/2$ and the steps at $\pm\nu_Q$ are the result of the first order +1/2 -> +3/2 and -3/2 -> -1/2 transitions corresponding to 90° and 0° orientations respectively. For stronger quadrupole coupling, the central peak begins to broaden due to the angular dependence of the energy levels and the second order correction for the -1/2 -> +1/2 transition is shown in Figure 1.1(b). The second order correction splits the central resonance into two

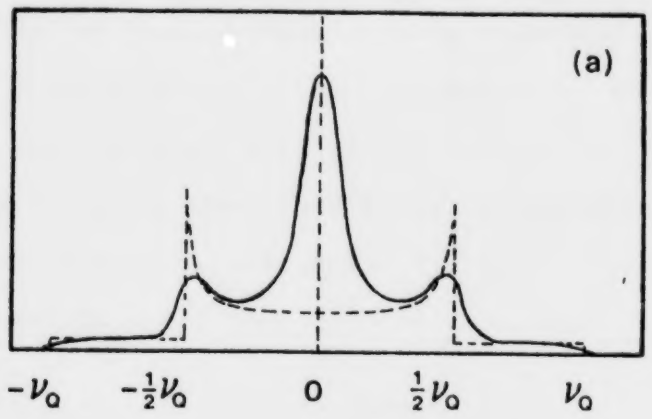

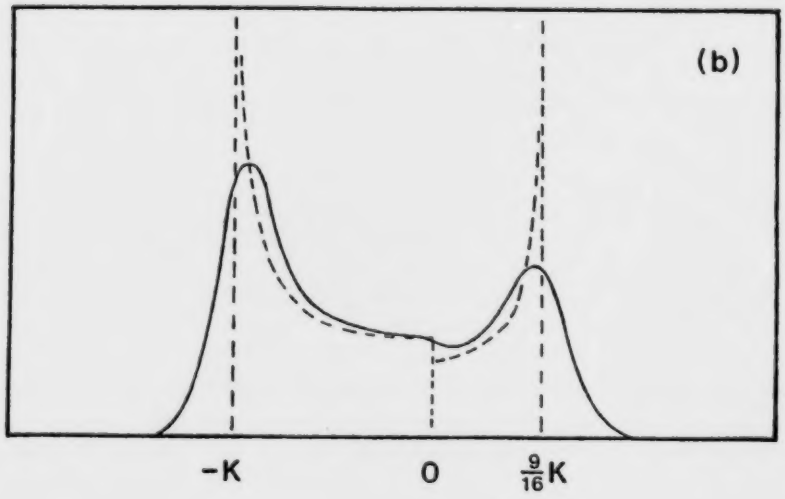

$$K = \frac{\nu_Q^2}{3\omega_o}$$

Figure 1.1(a)

Quadrupole powder patterns for spin 3/2. The powder patterns are centred about the Larmor frequency.
(Poole and Farach 1972)
(a) First order powder pattern
(b) Second order powder pattern

peaks, the separation of these peaks being proportional to ν_Q^2 / ν_L . As noted earlier, the important identifying characteristic of a second order quadrupole coupled resonance is that its width is inversely proportional to the magnetic field.

1.4 The effects of atomic motion on NMR

The nmr resonance will be affected by changes in its local environment. Such changes can be induced by changes in the static environment which may occur at a phase change or by the presence of more than one phase, by changes in the local lattice vibrational spectrum, or through effects related to ionic motion. Such effects are normally strongly related to the temperature of the material. Theoretical studies are based on the use of a time dependent Hamiltonian and a number of reviews have been published.(Richards 1979,Bjorkstam and Villa 1980).on this section we briefly review the principal theory of effects due to ion motion.

(a) The Bloembergen, Purcell and Pound (BPP) model

The principal assumption is that time dependent effects in the lattice can be characterised by a single exponential function of the form

$$\langle V_{zz_\alpha}(t)\, V_{zz_\alpha}(0)\rangle = e^{-t/\tau} \qquad (12)$$

where V_{zz} is as previously defined and α refers to all sites with different efg values and/or directions within the crystal. This is called the lattice correlation function, and the parameter τ is the lattice correlation time. τ is a measure of the time in which a change in the lattice occurs. This

function is applicable to fluctuations arising from any mechanism - molecular rotation or vibration, phonons, as well as ionic motion and may be used to calculate values for T_1 and T_2 . In calculating T_1, the important parts of the spectral density are at ν_L for $\Delta m = \pm 1$ and at $2\nu_L$ for $\Delta m = \pm 2$, where ν_L is the nmr frequency (eqn.4). For dipolar coupling

$$\frac{1}{T_1} = A \left[\frac{\tau}{1 + \omega^2 \tau^2} + \frac{2\tau}{1 + 4\omega^2 \tau^2} \right] \qquad (13)$$

where A is determined by the dipolar interaction strength. In the case of T_2, frequencies from zero to the frequency of the dipole interaction (approximately equal to the dipolar linewidth) contribute to the relaxation. Integrating over these limits gives

$$\left(\frac{1}{T_2} \right)^2 = (\Delta\omega_{RL})^2 \tan^{-1} (\tau/T_2) \qquad (14)$$

where $\Delta\omega_{RL}$ is the rigid lattice dipolar linewidth. A plot of the BPP results for T_1 and T_2 as a function of $\ln(\tau)$ is given in Figure 1.2. If, as is usual, τ is assumed to be thermally activated

$$\tau = \tau_o \exp(W/kT) \qquad (15)$$

where W is the activation energy, then a plot against $\ln(\tau)$ has the same form as a plot against 1/T. The results show that $1/T_2$ is constant until the frequency approaches the line width measured in frequency units, after which $1/T_2$ is proportional to

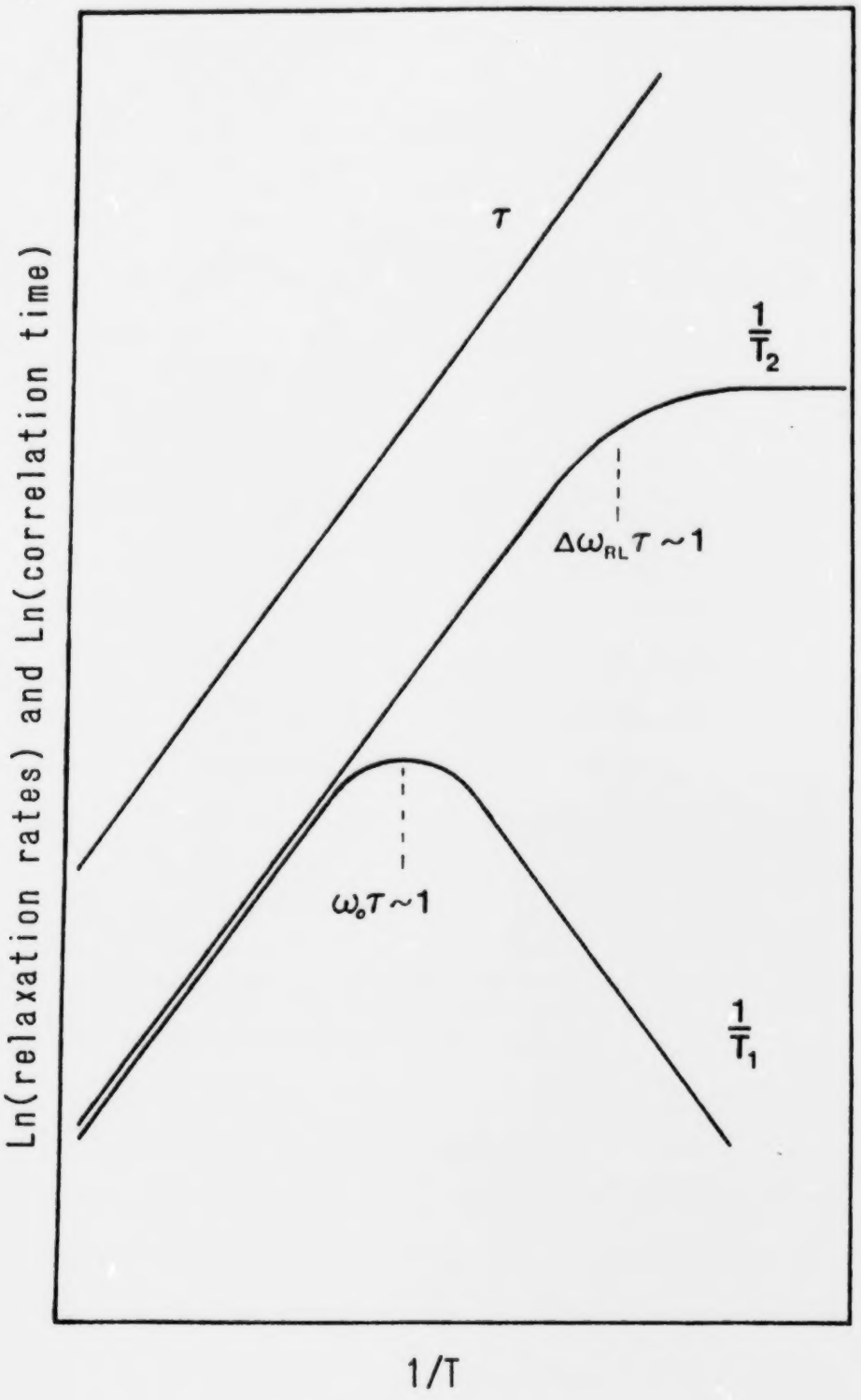

Figure 1.2

Results of BPP theory - Temperature dependence of the correlation time τ and the relaxation times T_1 and T_2.

frequency. Since $1/T_2$ is proportional to the dipolar linewidth, this predicts motional narrowing of the linewidth. The T_1 results are characterised by a minimum where the correlation frequency and the NMR frequency are the same. Thus from the BPP theory, it should be possible to estimate the correlation time τ by measuring T_1 , T_2 or the dipolar linewidth.

(b) Motional effects in quadrupolar coupling

Bjorkstam and Villa(1980) have shown that the first order quadrupole shifts are not dependent on atomic motion, but that second order shifts are. An exponential correlation function is again defined, and this leads to an expression for the second order quadrupole shift

$$\delta = B \left[\frac{\omega \tau^2}{1 + \omega^2 \tau^2} + \frac{2 \omega \tau^2}{1 + 4\omega^2 \tau^2} \right] \qquad (16)$$

where B is the strength of the quadrupole interaction.

The limits on T_1 and T_2 and δ at low and high temperatures assuming a thermally activated process for τ are summarised in Table 1. It may be noted that the quadrupole shift acts much like $1/T_2$ except that the decrease in δ starts at $\omega_L \tau \sim 1$, the same point as the T_1 minimum. However, at low τ (high temperature), δ varies as τ^2 whereas T_1 and T_2 vary as τ . This summary will be employed to interpret the experimental results in later sections.

BPP

$1/T_1$	$\propto \tau$	$\omega\ \tau << 1$	high T
	$\propto \omega^{-2}\tau^{-1}$	$\omega\ \tau >> 1$	low T
$1/T_2$	$\propto \tau$	$\Delta\omega_{RL} << 1$	high T
	constant	$\Delta\omega_{RL} >> 1$	low T

QUADRUPOLE COUPLING

δ	$\propto \omega\ \tau^2$	$\omega\ \tau << 1$	high T
	$\propto \omega^{-1}$	$\omega\ \tau >> 1$	low T

TABLE 1: Limits of nmr parameters at low and high temperatures assuming a thermally activated lattice correlation time

1.4 The relationship between nmr and ionic conductivity

The ionic conductivity σ is expressed in terms of the diffusion coefficient D through the Nernst-Einstein equation

$$\sigma = \frac{n (Ze)^2 D}{kT} \qquad (17)$$

where n is the density of carriers, Ze is the carrier charge. Using the simplest isotropic hopping model involving a thermally activated process between sites separated by distance l with an attempt-to-escape frequency ν_o, the diffusion coefficient D is

$$D = \frac{\nu_o l^2}{6} \exp(-W/kT) \qquad (18)$$

This leads to an expression for the conductivity of the form

$$\sigma = \frac{n (Ze)^2 l^2 \nu_o}{6kT} \exp(-W/kT) \qquad (19)$$

and the activation energy W can be measured from the slope of a graph of $\ln(\sigma T)$ versus $1/T$.

The process can be related to nmr through the lattice correlation time τ. As noted earlier, τ is the mean time for a change in the lattice surroundings to occur. The process of ionic hopping is changing the local environment of a given lattice site at a rate ν_o. If there is no other motion - such as molecular rotation- then the lattice correlation time should be the reciprocal of the hopping frequency. On this basis, the conductivity should be calculable from T_1, T_2 and the dipolar and quadrupolar linewidths. It is this relationship that has been one of the interests in the present work.

2. EXPERIMENTAL

The experiments undertaken involve the following areas:

(a) Nuclear magnetic resonance

(b) Conductivity measurements using ac impedance

(c) Sample fabrication for NYS and NGS

2.1 NMR Spectrometer

The NMR spectrometer used in most of these experiments was a broad line induction spectrometer of a design described by Torgeson (1967). Varian probes were used and a range of frequencies from 2.5 to 25 MHz was available. The magnet was a 15 inch Magnion magnet capable of producing fields of up to 2.2 Tesla. Resonances were measured using the technique of non-adiabatic rapid passage and a schematic of the experiment is shown in Figure 2.1. Special coils were used to ramp the magnetic field at a frequency of about 20 Hz. The NMR signal was fed directly into a NICOLET 1170 signal averager. Magnetic field sweeps up to 400 gauss were possible. The advantages of non-adiabatic rapid passage are discussed by Segel and Mansingh (1969). In cases where the resonance was at a low frequency, very low intensity or was very broad, standard slow passage NMR was used because it resulted in a smoother baseline. For this technique, the field was swept at a rate of about 1 Hz; the output of the spectrometer was fed through a phase sensitive detector and then into the signal averager; and a modulation field was applied through the

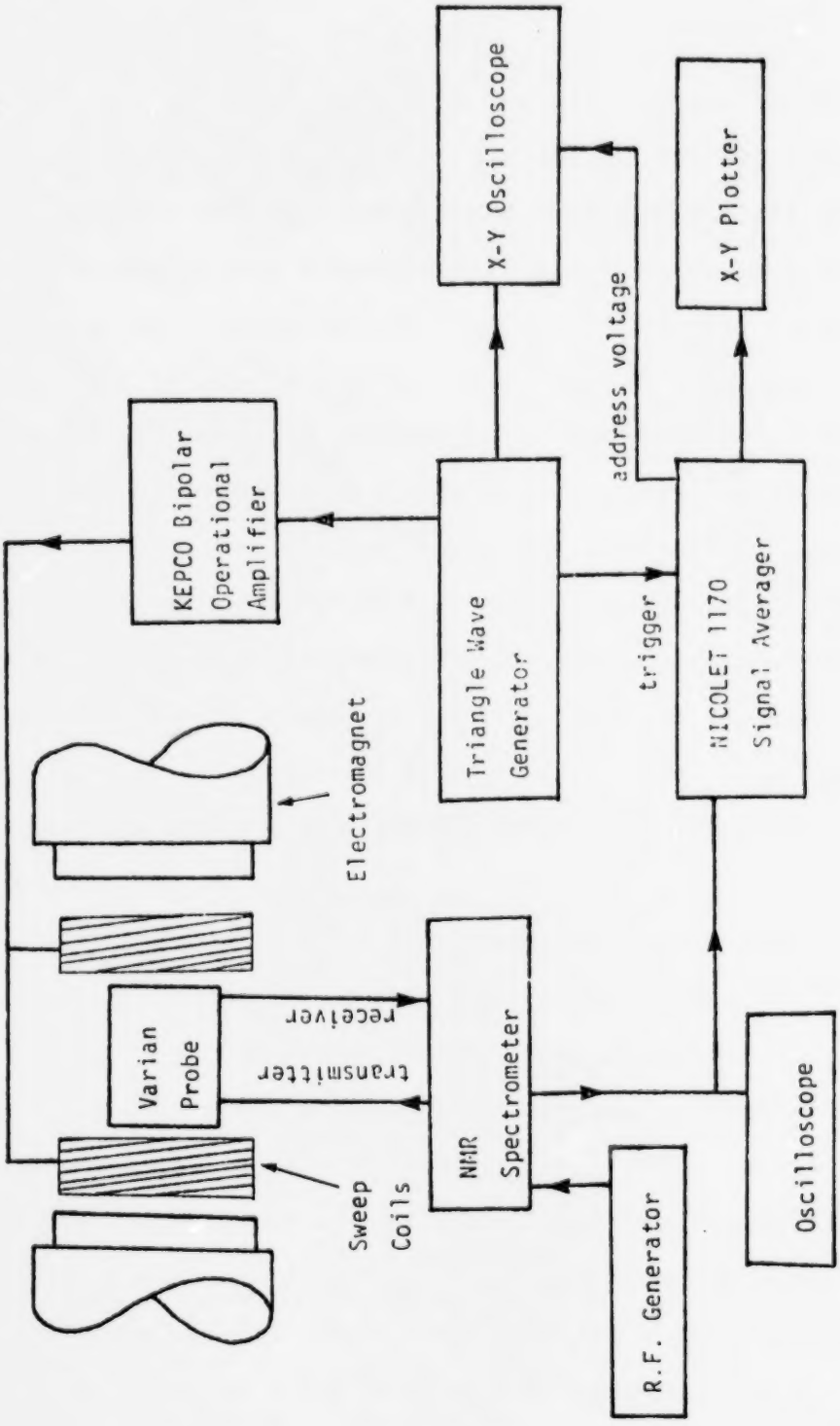

Figure 2.1

A schematic diagram of the fast-passage NMR experiment.

modulation coils in the Varian probe. Again, field sweeps up to 400 gauss were used. Resonances were accumulated by signal averaging over periods ranging from 1 to 60 minutes depending on the signal intensity. The accuracy of measuring linewidths was typically ± 10%. NMR spectra taken at 5 Tesla were measured using a Bruker CXP 200 Pulsed NMR - Fourier Transform Spectrometer located in the Department of Chemistry.

A particular aspect of this work was the use of the spectrometer at relatively high temperatures (< 300 C). A quartz dewar pipe was fixed inside the Varian probes (quartz was used because it did not contain sodium). Samples were wrapped in teflon tape, fixed to the end of a mullite rod and inserted into the dewar pipe. A thermocouple was placed about 1 mm away from the sample. For heating above room temperature, air was passed through a heater and then through the dewar pipe. For cooling samples, nitrogen gas, resulting from the boil off of liquid nitrogen, was passed through the dewar pipe and temperatures as low as 150 K could be obtained. The accuracy of this temperature measurement was ± 2 C.

2.2 Conductivity measurements

Conductivity measurements were made using ac impedance methods (Bottelberghs 1978). An automated conductivity measuring apparatus built by D.S.Smith and M.F. Bell (Smith 1982), was used to measure ionic conductivity. A diagram of the measuring system is shown in Figure 2.2. The core of the automated system is a 4016 Commodore PET computer

which controls all the measurements. A Hewlett-Packard 3575A gain-phase meter measures the ratio of the amplitudes and phase difference between the voltages across the measurement cell and the standard resistance, and presents this information to the PET. The PET then calculates the impedance of the cell. The frequency generator is controlled by the PET and a complete impedance plot can be measured automatically and either stored on floppy disk or outputted onto a printer. The PET controls the oven temperature by means of a Thermoline controller, and measures the sample temperature with a thermocouple and an IEEE compatible digital voltmeter. Conductivity measurements were usually taken from room temperature to 350 C and the accuracy of the temperature measurement was about ± 2 C. The repeatibility of the conductivity measurements was ± 20%.

2.3 Materials Preparation

All NYS and NGS samples were fabricated by a spray freeze/freeze dry process by P.S.Nicholson of McMaster University (Bentzen and Nicholson 1980). Eight Nazirpsio samples from three different sources were employed - from the Ontario Research Foundation(ORF), from M.F.Bell (HB), and six samples from T.A.Wheat(CANMET). The CANMET samples ranged from $x = 1.8$ to $x = 2.3$ and were monoclinic in structure for $x = 1.8, 1.9, 2.0$ and rhombohedral for $x = 2.1, 2.2$ and 2.3. β -alumina samples were also acquired from a variety of sources with a range of densities and fraction of the β phase.

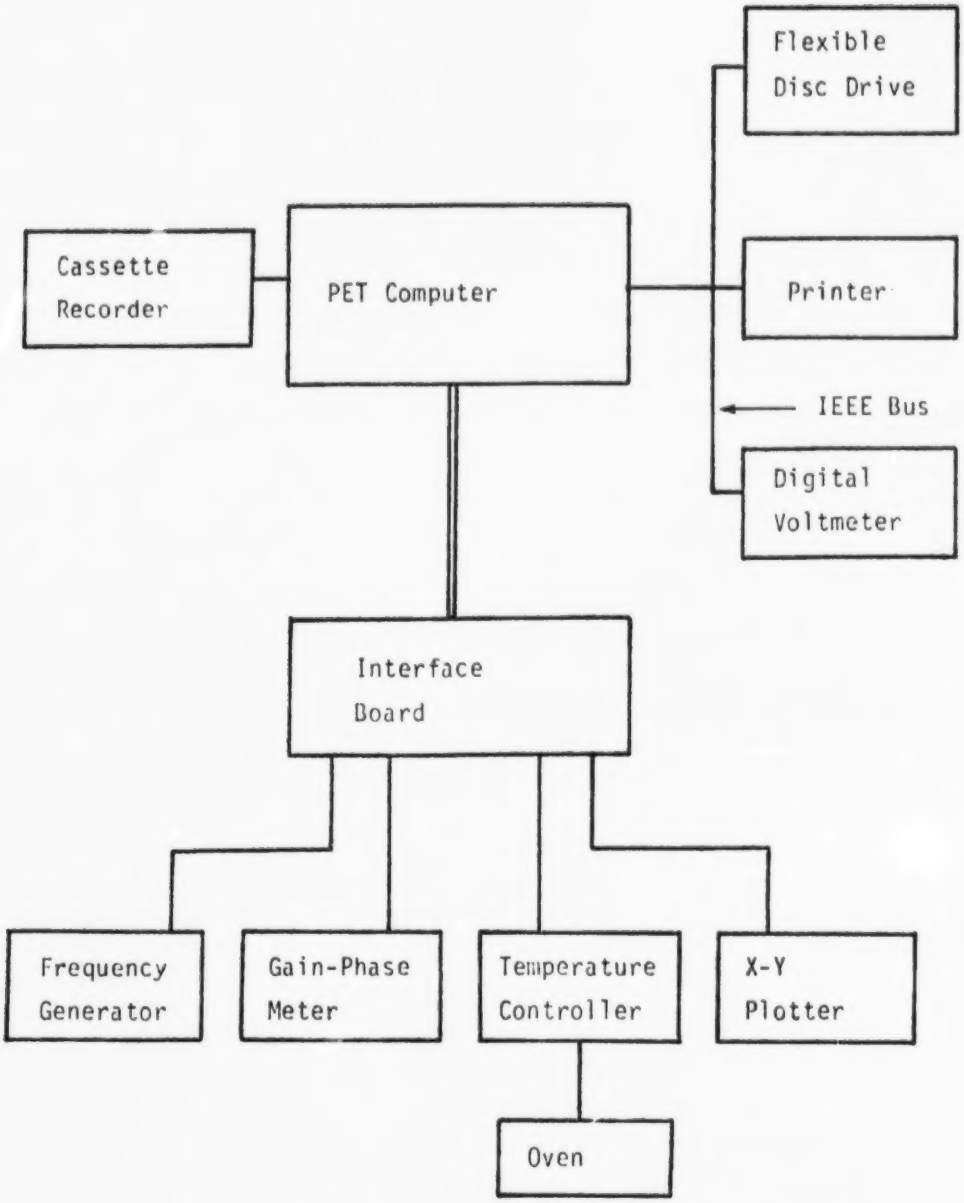

Figure 2.2

Schematic of automated a.c. conductivity apparatus.

2.4 Sample preparation

For electrical measurements the samples of Nazirpsio, NYS and NGS were cut such that the geometric factor, length divided by area, ranged from 3 to 7 cm^{-1}. The ends of the samples were polished and platinum paint contacts were applied (Englehard Liquid Bright Platinum fired at 300 C). Humidity has been shown to affect the conductivity of other sodium ion conductors (Will 1976), so in order to avoid water absorption effects, all the samples were dried overnight in an oven at 200 C and stored in a desicator until they were ready to be used.This procedure was also employed prior to measurements of nuclear magnetic resonance. The voltage across the samples was kept under 20 mV and was typically 5 mV peak to peak. This was necessary to keep the current low during the measurement to avoid irreversible electrode changes and heating effects (Bauerle 1969). Examples of the impedance plots for a Nazirpsio x=1.9 sample at two different temperatures are given in Figure 2.3. For all the samples measured in this work, the high frequency intercept with the real axis was taken to be the bulk value of the ionic conductivity (von Alpen et al 1979).

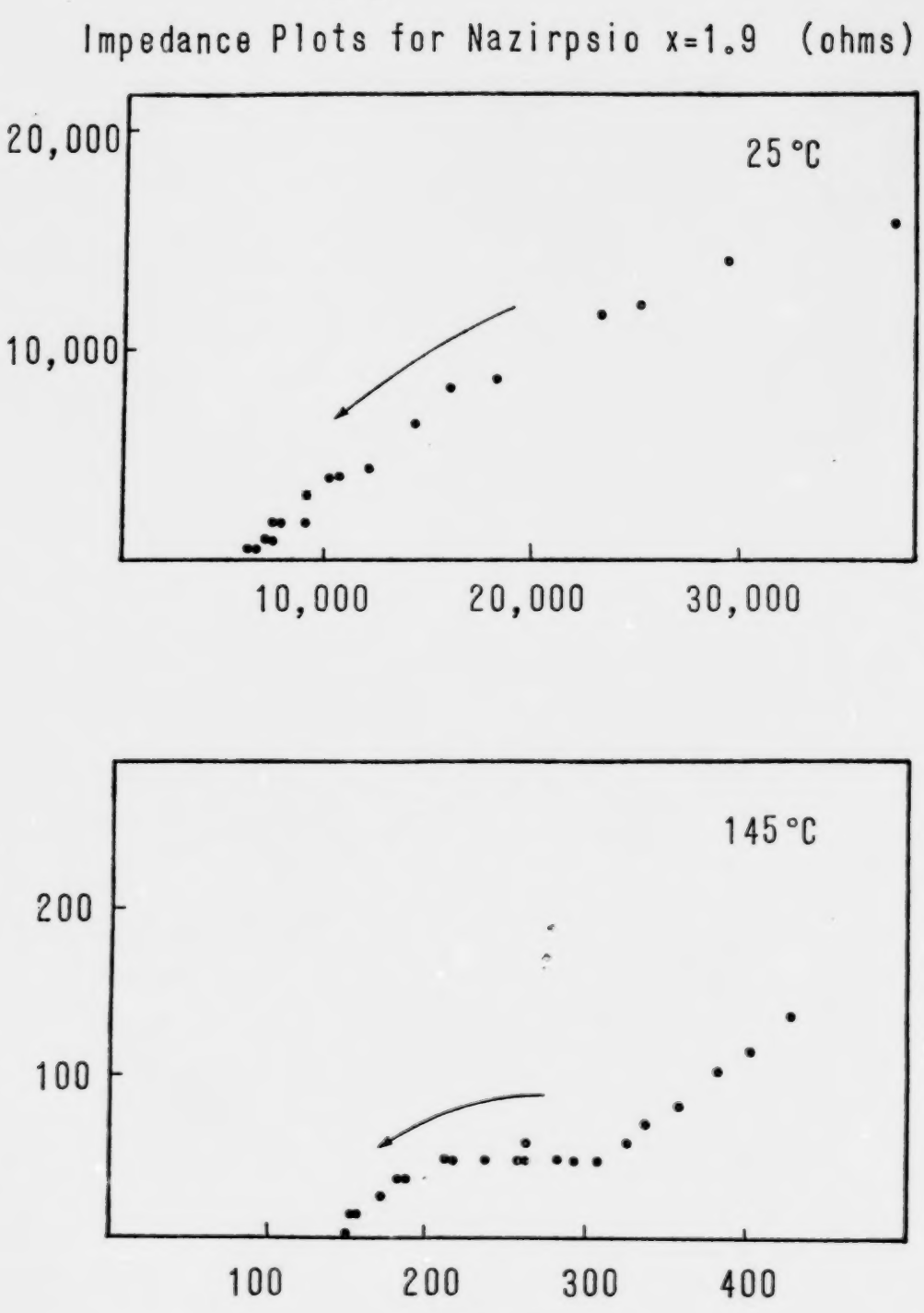

Figure 2.3

Typical impedance plots for Nazirpsio. The arrow indicates the direction of increasing frequency.

3. RESULTS

The measurements reported are as follows:

1. Na β -β" Aluminas - showing qualitative effects of differing proportions of the β phase.
2. Nazirpsios of varying composition
3. NYS
4. NGS

3.1 Na β - β " Aluminas

The largest amount of nmr work published on fast ion electrolytes has been carried out on Na β and β " aluminas, primarily in the form of single crystals (Chung, Story and Roth 1975,Bailey et al 1976,Bjorkstam, Villa and Frye 1981. Figure 3.1 shows results for a number of polycrystalline samples from various sources, with the temperature dependence of the conductivity being given in Table 3.1 and Figure 3.2. The f(β) of each sample, defined as the fraction of the material in the βphase, is also given in Table 3.1.

A significant variation in the resonance shape is observed between samples sufficient to distinguish between them on a routine basis. A small part of this variation could have been due to the presence of water in the lattice(Kline,Story and Roth 1972) ,although the line shapes indicated that the samples were essentially dry. However, the most significant reason for the varying line shapes appeared to be f(β), the proportion of the β and β " phases present. The electrical data in Figure 3.2 shows that all samples have similar conductivity

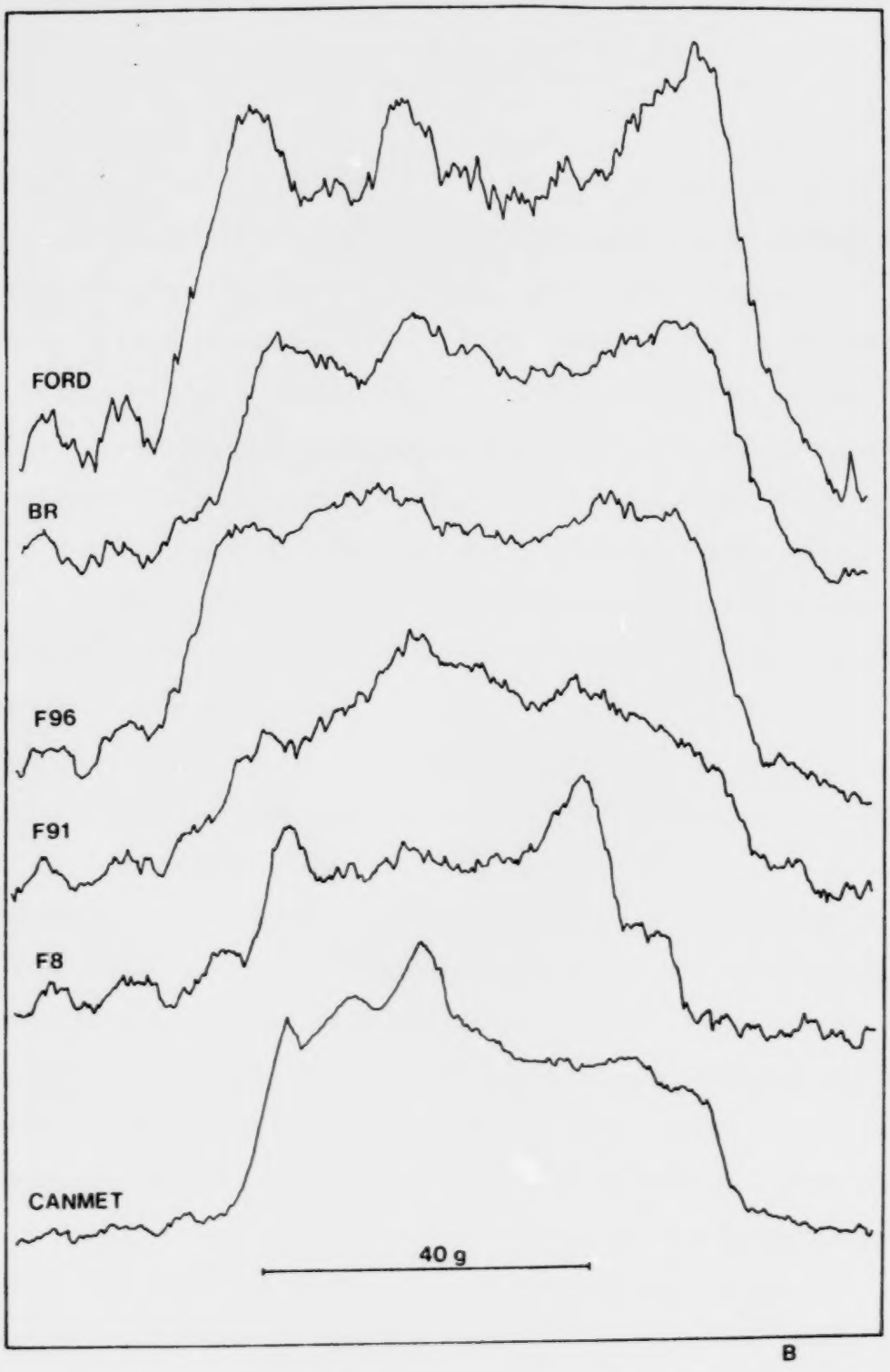

Figure 3.1 NMR of Na$_2$O" aluminas from various sources

Source	f(β)	$(\sigma\text{-cm})^{-1}$
Ford	0	0.25
British Rail	0.07	"
ORF F96	0.245	"
ORF F91	0.38	"
ORF F8(Li-7)	1.0	0.05
CANMET	0.47	0.25

Table 3.1 f(β) and conductivity at 300 C for polycrystalline β-aluminas from various sources.

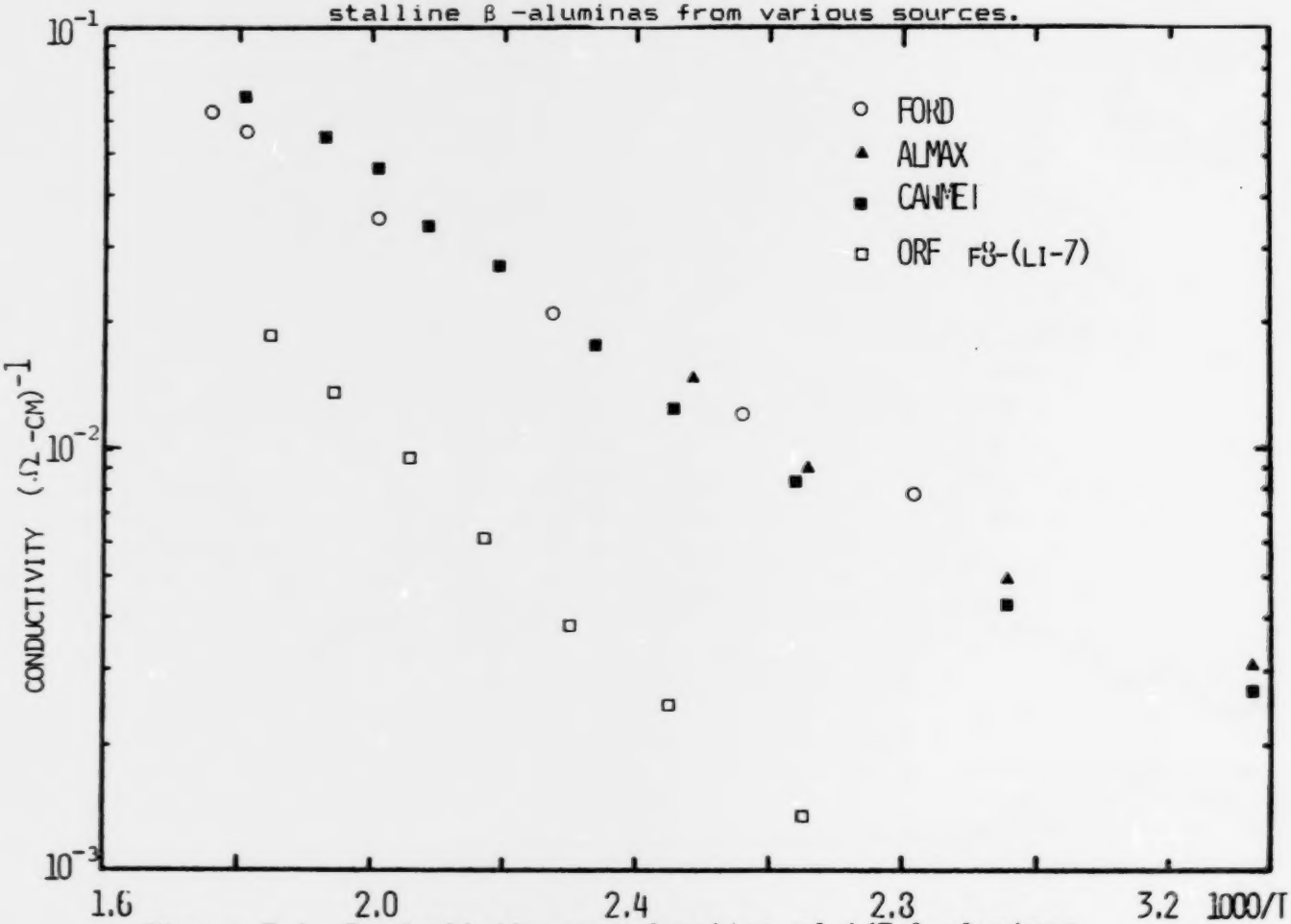

Figure 3.1 Conductivity as a function of 1/T:β-aluminas

(Measurement by D.Smith and M.F.Bell 1982)

except #1 which is 100% β phase (f(β)=1). No direct correlation was apparent between the magnitude of the conductivity and the nmr resonance lineshape or intensity. The temperature variation of the resonance observed in material # F8 (Li-7) was investigated in detail up to 100 C. Although dipolar narrowing was observed, there was no evidence for changes in quadrupole broadening or frequency shifts as previously reported by Bailey et al (1972). It is not clear why these discrepancies occur, although it is consistent with a range of observations which have been reported in the literature. At present the evidence is clearly sample dependent.

3.2 Nazirpsios

The sodium resonances from the range x=1.8 to x=2.3 in the formula $Na_{1+x}Zr_2P_{3-x}Si_xO_{12}$ were measured at 23 MHz and at room temperature. Sample spectra at the ends of this range are shown in Figure 3.3. The resonances are broad and featureless. The peaks of the resonances are shifted slightly to the high field side of the free ion frequency. This shift decreases with increasing x. The resonance at x=2.3 is almost symmetric but gradually becomes more asymmetric as x decreases. Because there is no structure, the parameter chosen to characterize the resonances was the full width at half the maximum height (FWHM). At room temperature, the resonance widths are 16 to 18 gauss FWHM at 23 MHz and no difference was noticed between the CANMET, ORF or HB samples of the same x. The resonances were then observed as a function of magnetic field at room

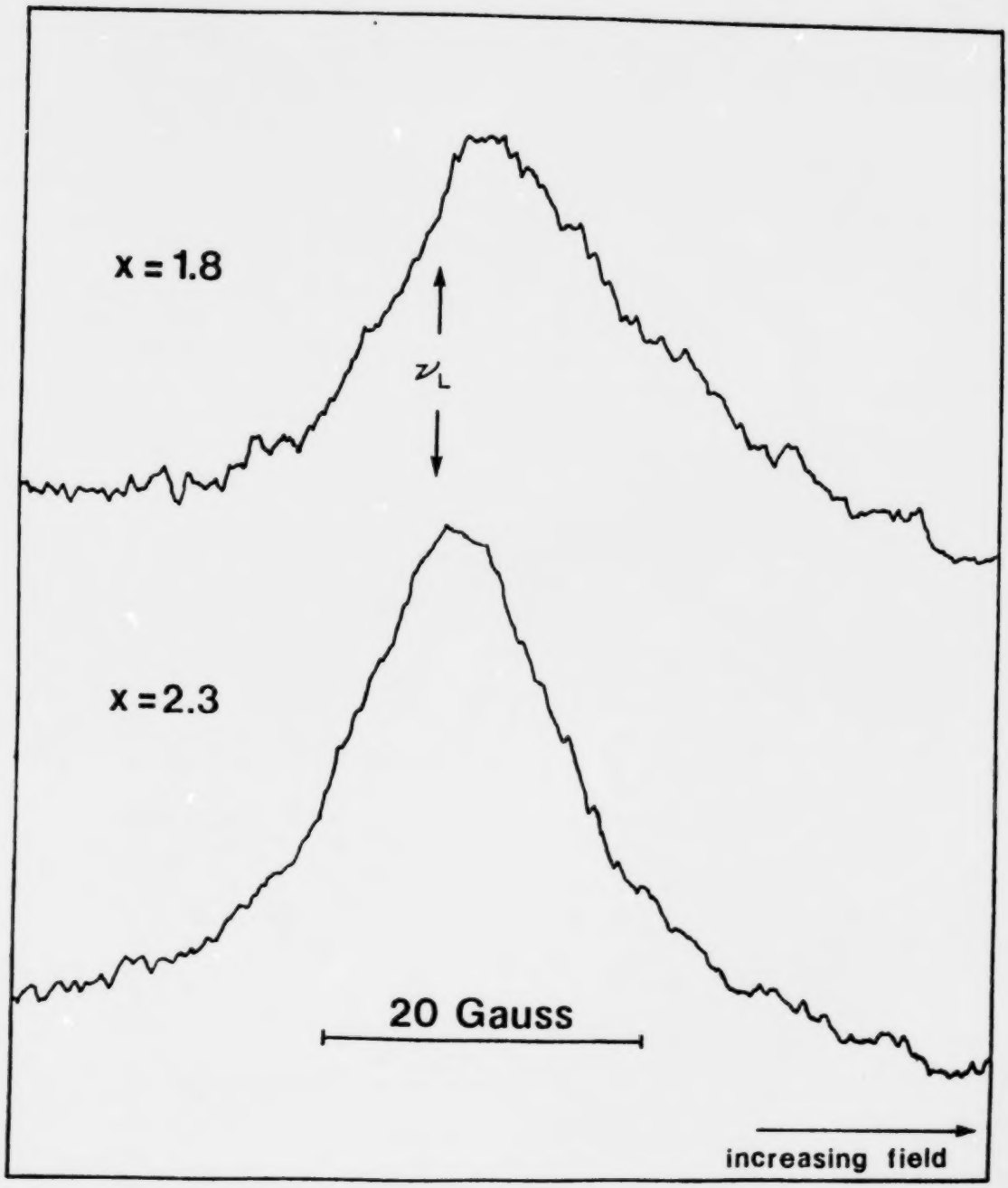

Figure 3.3

Typical sodium resonances for Nazirpsio x = 1.8 and x = 2.3 at room temperature and 23 MHz.

temperature. There was no change in the shape of the resonances at different fields, just in the width. The results for the HB x=1.9 sample are given in Table 3.2 and show that the product of the linewidth and magnetic field is constant. This implies that the width varies inversely to the magnetic field -a characteristic of a second order quadrupole coupled resonance. This is reasonable even though there is no structure such as that shown in Figure 1.1 because there is more than one crystal site for the sodium atoms. X-ray analysis shows that there are three inequivalent sodium sites, and in addition, because there are more sites than sodium atoms, sodium vacancies will affect the long range quadrupole interaction. Therefore, the sodium resonance of Nazirpsio arises from the overlap of at least three of the simple quadrupole patterns and superimposed dipolar coupling and it is not surprising that no structure is observed. The resonances have more weight to the high field side of ν_L which is also in agreement with the postulate of second order quadrupole coupled resonances. This conclusion was found to be valid for all samples at room temperature. The samples supplied by CANMET were small and long signal averaging times were required. Because of this, the initial investigation and the most thorough work was done on the largest sample, HB x=1.9. The sodium resonance of this sample was measured as a function of temperature and magnetic field. As the temperature increased, the linewidth began to narrow as in Figure 3.4. The three main

Field H (MHz)	Linewidth (gauss)	Field x Linewidth (MHz)	T(1/2) (K)
6.22	55	0.39	373
10.54	37	0.44	377
22.6	16	0.41	403
52.9	6.3	0.38	416
.05	10	10	2 +%

Table 3.2: Nmr data for Nazirpsio HB (x=1.9) at 25 C

Source	"x"	Nmr ActivationEnergy (eV)	T(1/2) (K)
CANMET	1.8	0.37	398
	1.9	0.42	406
	2.0	0.30	411
	2.1	0.23	360
	2.2	0.20	356
	2.3	0.19	343
ORF	2.0	0.40	379
HB	1.9	0.31	403
		.04	5 ±

Table 3.3: Nmr parameters of Nazirpsios from various sources at 2 T.

points to note are that the resonance narrows, becomes symmetric and the peak moves towards ν_L . A graph of the linewidth as a function of temperature is given in Figure 3.5. The linewidth is constant up to 320 K and narrows to 2.5 gauss at 450 K. This narrowed resonance at high temperature may be broadened slightly by the imhomogeneity width resulting from non-uniformity of the magnetic field which is about 1.0 to 1.5 gauss. The data was then graphed on an Arrhenius plot as the natural logarithm of the linewidth against inverse temperature. The complete results for the field and temperature studies of the HB x=1.9 sample are shown in Figure 3.6. The line narrowing does follow an Arrhenius relation in that the high temperature segments are straight lines from which activation energies can be extracted. The activation energies have a modest and barely significant field dependence except for the data at 52.9 MHz. (The magnetic field strength is quoted equivalently in MHz or Tesla by using the gyromagnetic ratio for sodium, 11.2622 MHz/Tesla.) An unexpected feature of the data in Figure 3.6 is that the linewidth is independent of the magnetic field in the high temperature region, at least to the accuracy of the experiment. It appears that the second order quadrupole coupling has disappeared. T(1/2), the temperature where the linewidth is half that of the low temperature limit, was chosen as a measure of the onset of line narrowing. The values of T(1/2) for HB x=1.9 are given in Table 3.3. and it is seen that T(1/2) increases with increasing magnetic field. The

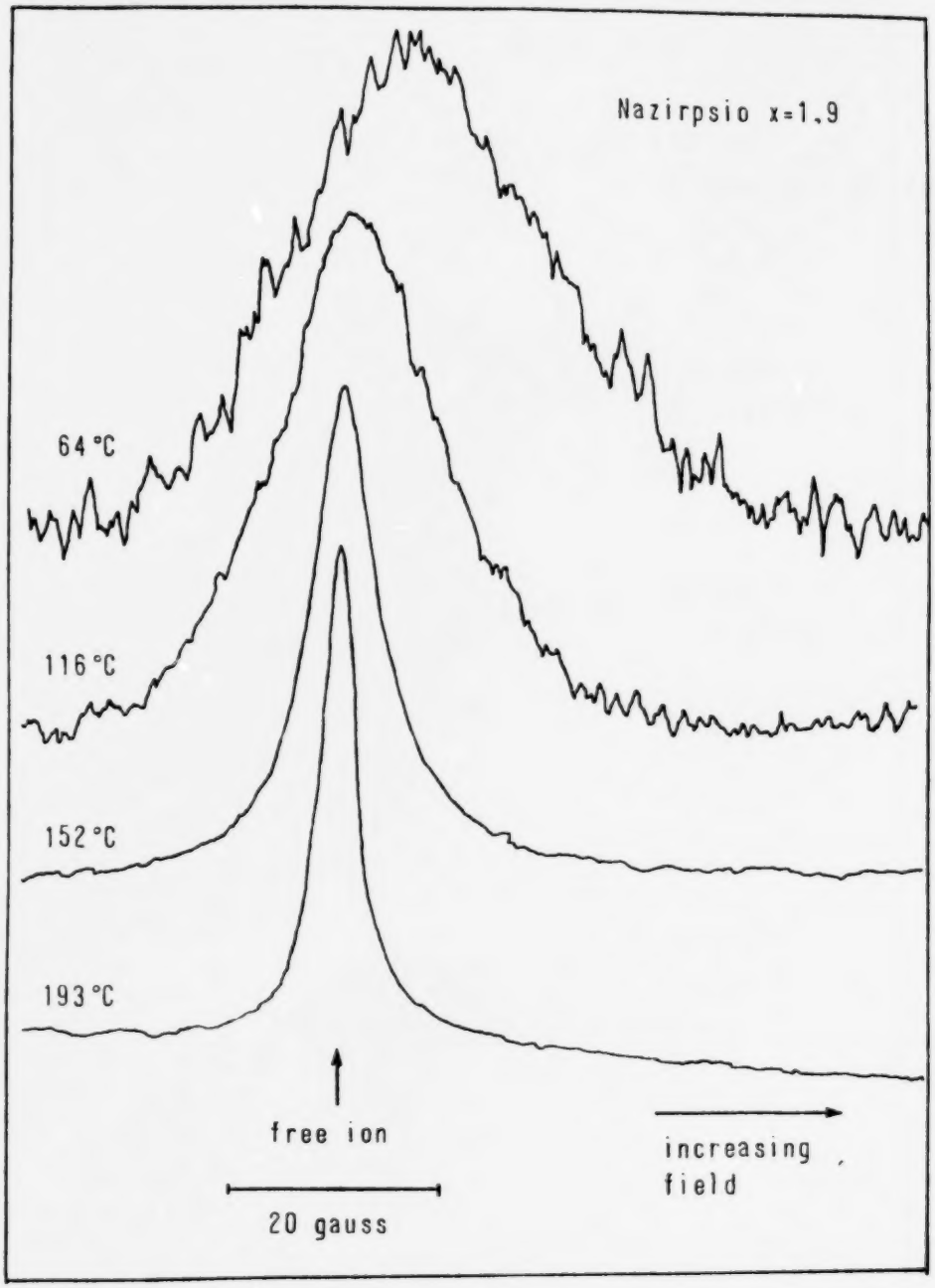

Figure 3.4

The change in the sodium resonance of Nazirpsio x = 1.9 with temperature at 10.5 MHz.

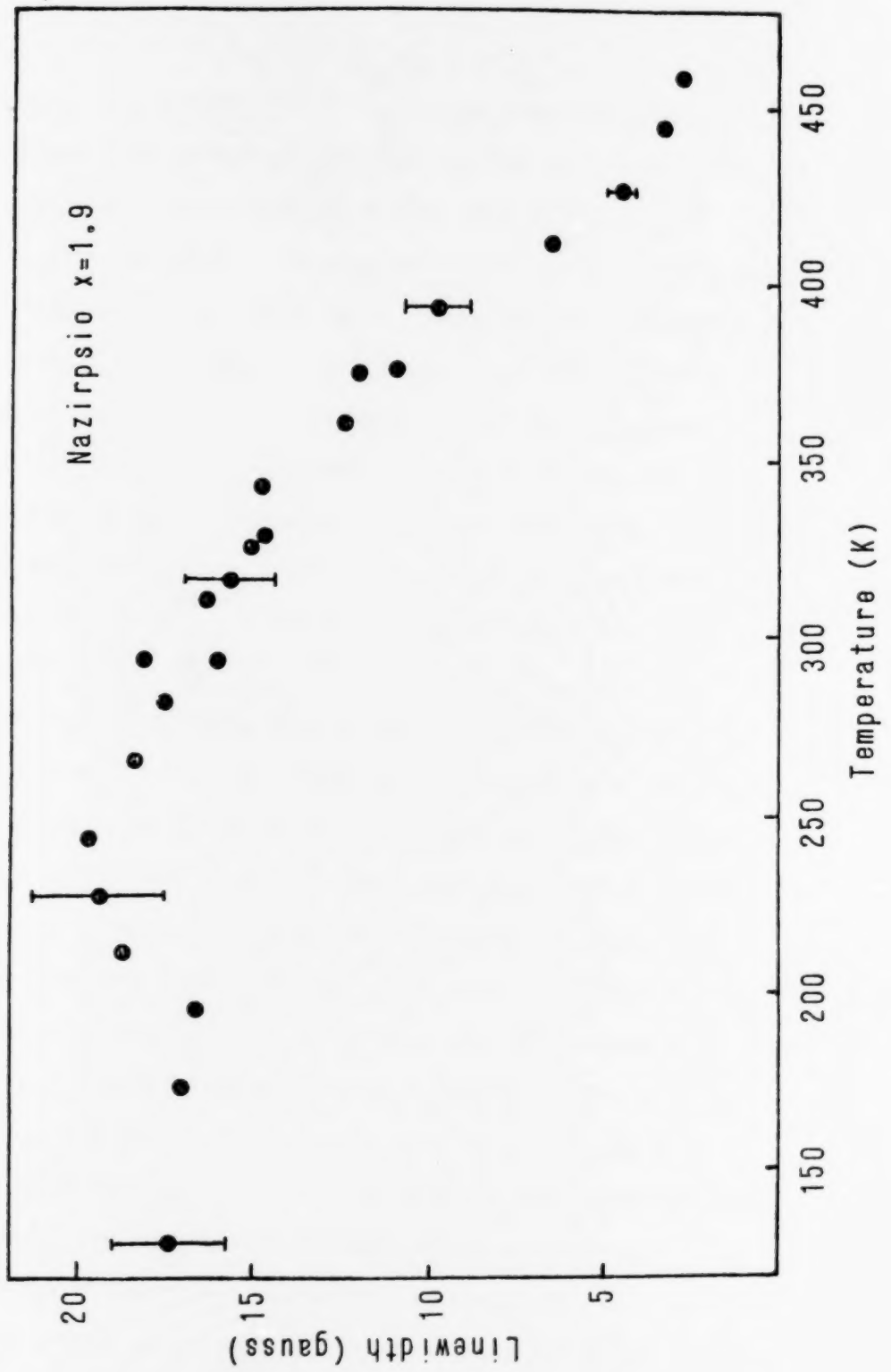

Figure 3.5

FWHM of Nazirpsio x = 1.9 sodium resonance as a function of temperature at 23 MHz.

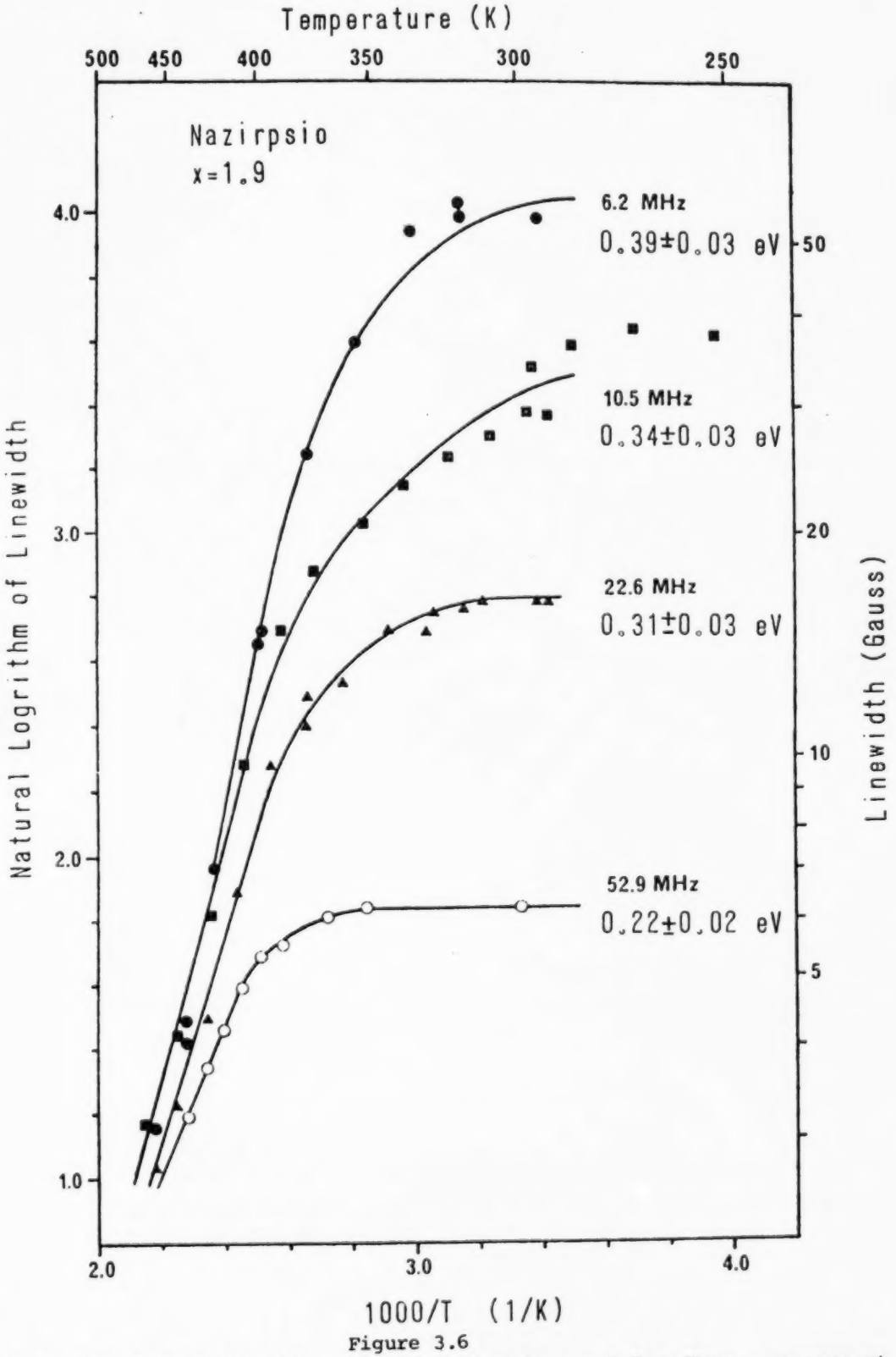

Figure 3.6

Arrhenius plot of the linewidth of Nazirpsio x = 1.9 sodium resonance at four different magnetic fields. The activation energies were derived from the slopes of the high temperature data.

seen that T(1/2) increases with increasing magnetic field. The BPP theory shows that onset of motional effects occurs when the correlation frequency is equal to either the interaction frequency,ie. the linewidth, or the NMR frequency. Since the correlation frequency increases with temperature, the onset of narrowing effects in Nazirpsio depends on the NMR frequency. If the onset of motional effects depended on the linewidth, T(1/2) would increase with decreasing field because the linewidth increases with decreasing field. Therefore the onset of narrowing occurs at the location of the T_1 minimum where $\omega\tau$ =1 even though the data in figure 3.6 is similar to a $1/T_2$ plot shown in Figure 1.2.

The line narrowing was studied for all the Nazirpsio samples at 10 and 23 MHz. All the samples behaved similarly to HB x=1.9 and there was no significant change in the activation energy between these two fields except for the CANMET x=2.0 sample. For this sample, the activation energy changed by a factor of two between 6 and 23 MHz. For all the samples, the activation energies calculated at 23 MHz and the onset of narrowing, T(1/2), are given in Table 3.3 and Figure 3.7. Generally, both the activation energy and T(1/2) gradually decrease with increasing x and have a sharper decrease between x=2.0 and x=2.1 (the monoclinic-rhombohedral boundary). Searches to find first order satellite peaks, the -3/2 to -1/2 and 1/2 to 3/2 transitions were not successful at either room temperature or 200 C.

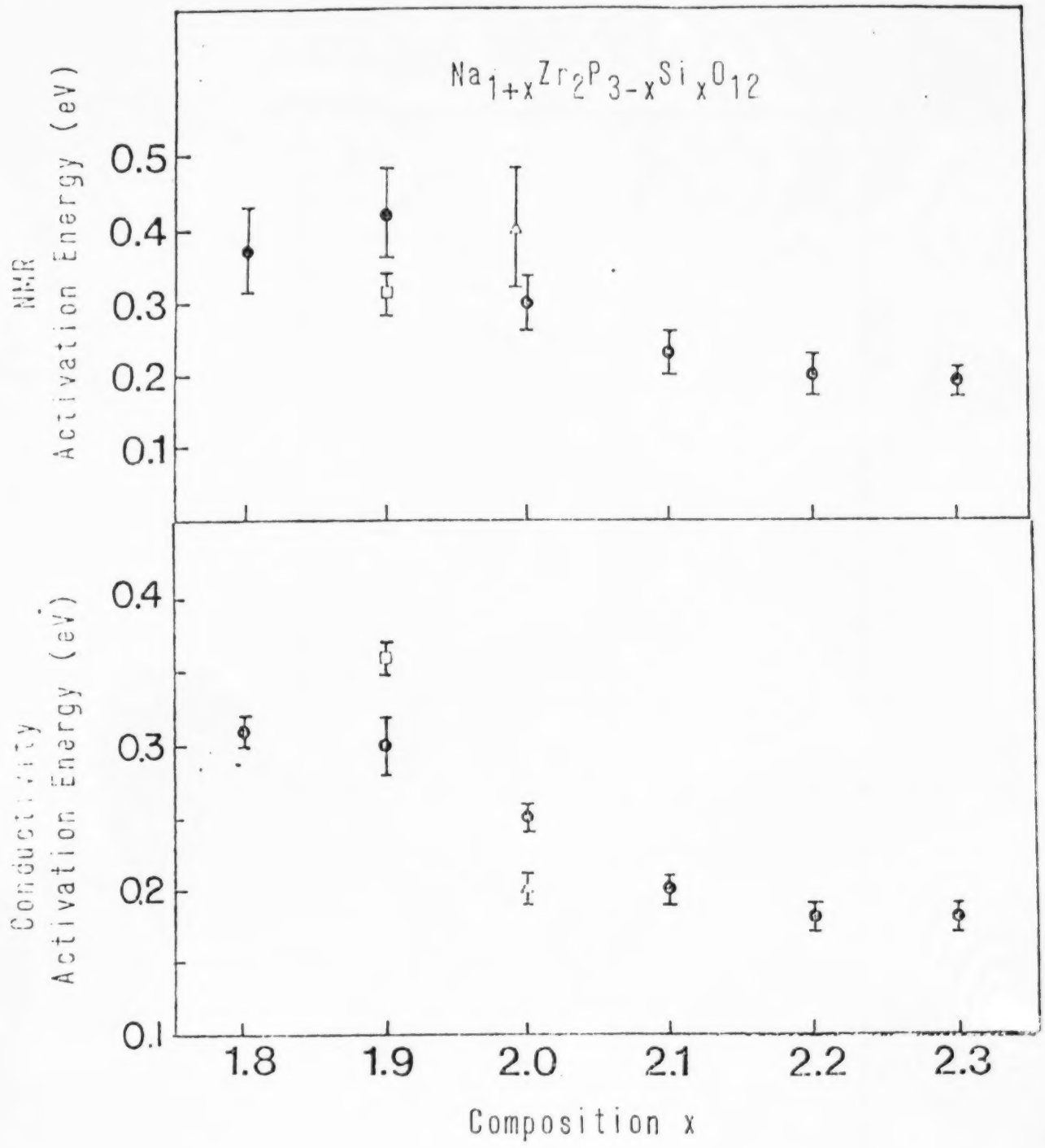

Figure 3.7

Activation energies calculated from NMR and conductivity as a function of composition.

3.2.1 Correlation between nmr and conductivity for Nazirpsio

The bulk conductivities of the Nazirpsios were measured from 20 to 350 C. Arrhenius plots for two representative samples are shown in Figure 3.8. The change in activation energy that occurs in the range 150 C to 200 C has been reported previously (von Alpen et al 1979) and has been shown to result from a monoclinic to rhombohedral phase transition. This explanation is consistent with the present results since the materials which were rhombohedral at room temperature only showed a single activation energy although the CANMET and ORF samples showed only one activation energy even though they were monoclinic at room temperature. The activation energies for different x and the conductivity at 300 C are listed in Table 3.4 and in Figure 3.8. There is a noticeable similarity in the trend of the activation energy with x for the nmr and the conductivity results. The activation energies are in agreement with those reported by von Alpen(1981) and Kafalas and Cava(1979). The values of the conductivity at 300 C are about a factor of 4 below published values for x=2, but agree within experimental error with measurements made on the HB (x=1.9) sample at the Max Plank Institute by M.F.Bell. This suggests that the conductivity variations do arise from compositional effects and sample preparation.

In Table 3.4 the measured bulk conductivity and activation energy is compared with that calculated and measured

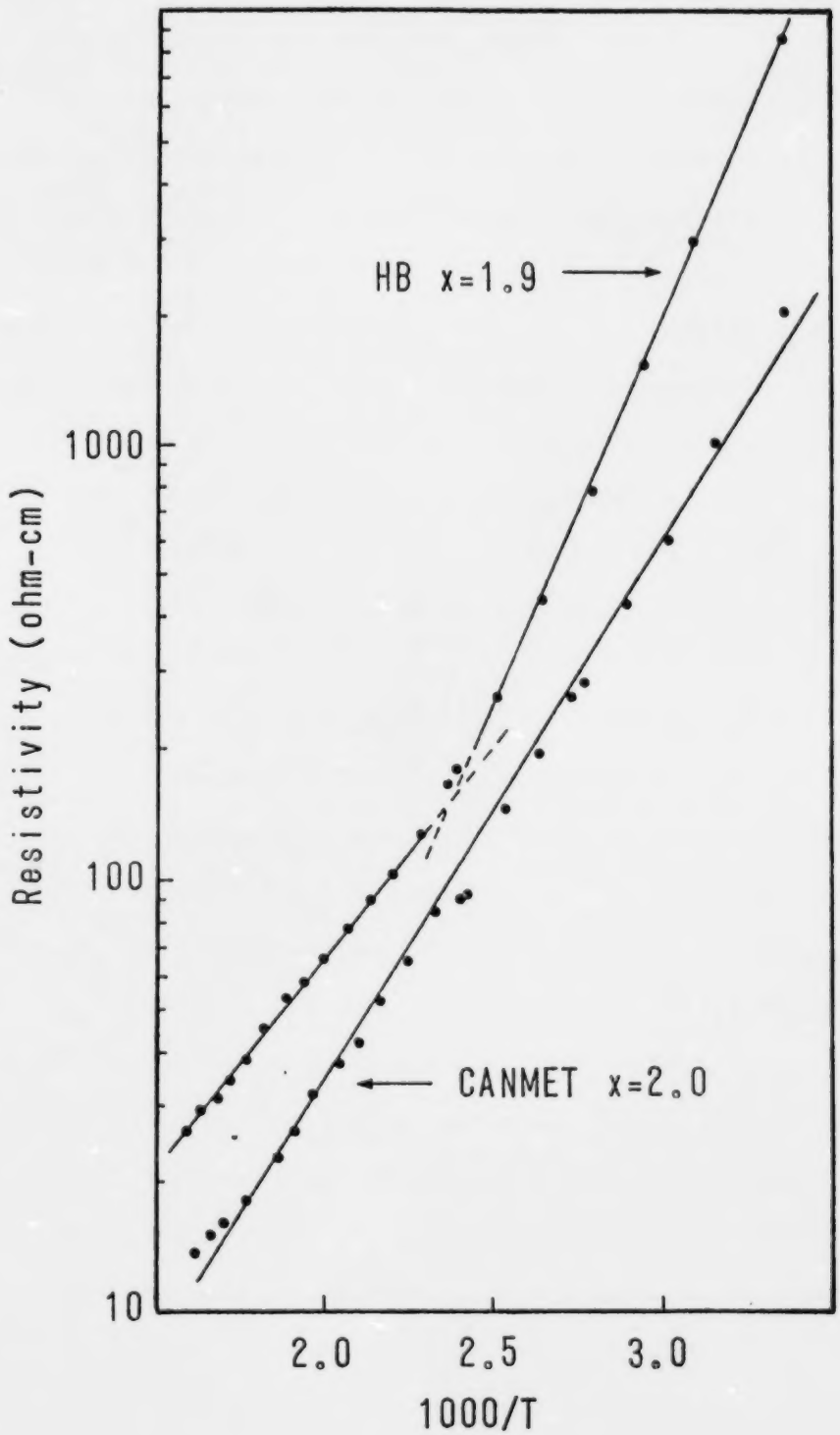

Figure 3.8

Resistivity of Nazirpsio. Some Nazirpsio samples had two activation energies as in HB x = 1.9 and others had one as in CANMET x - 2.0.

Source	"x"	Activation energy(eV)			Conductivity(σ-cm)$^{-1}$	
		cond.	nmr	log Hz	cond.	nmr
CANMET	1.8	0.31*	0.37	12.8	0.05	-----
	1.9	0.30*	0.42	13.4	0.06	-----
	2.0	0.25	0.30	11.9	0.06	0.011
	2.1	0.20	0.23	11.4	0.08	0.016
	2.2	0.18	0.20	11.0	0.06	0.012
	2.3	0.18	0.19	11.0	0.04	0.013
ORF	2.0	0.20	0.40	13.5	0.04	0.070
HB	1.9	0.36*	0.31	11.9	0.03	-----
uncert:		.01	.04	.6	.01	.005

Table 3.4 Comparison of activation energy and conductivity at 300 C determined from ac conductivity and nmr for Nazirpsios

Samples marked * have a second high temperature activation energy as follows

CANMET x=1.8,0.14;x=1.9,0.20 HB x=1.9,0.19eV

respectively from Nmr data. The attempt-to-escape frequency ν_o has been estimated assuming that the hopping frequency is equal to the nmr frequency at temperature T(1/2) and the conductivity was calculated from eqn.19 using the mean lattice site spacing of 3.73 A for Nazirpsio, the nmr activation energy, and a value for n computed from the stoichiometry of the composition. Since the nmr measurements were made at the temperature T(1/2), which was of the order of 100 C, the results had to be extrapolated to 300 C. Materials which showed a change in activation energy were therefore excluded from the calculation.

The measured and calculated conductivities agree within a factor of 5 in all cases - a remarkable situation given the number of assumptions made in the development of the nmr calculation. The agreement is less notable if the published conductivities at 300 C are assumed to be 'correct'. However, there appears no reason to believe that the conductivities of the CANMET samples are not those measured, and that the nmr is not characteristic of the particular material preparation. It maybe noted that the attempt-to-escape frequencies for the rhombohedral samples are about an order of magnitude higher than those for the monoclinic phases, and are less than might be expected from optical phonon frequencies, 10E13 Hz. However, this has been noted in other nmr measurements (Richards 1979) and ν_o is also known to be lower than 10E13 in other crystalline and glassy systems (Mansingh et al 1980).

One sample is anomalous in these measurements. The ORF x=2.0 sample shows a factor of two difference between nmr and conductivity activation energies and has an activation energy measured in nmr which is apparently field dependent. Although the calculated and measured conductivity at 300 C is in agreement, this appears fortuitous. As noted below, this sample was also unique in its P^{31} resonance. It therefore appears that the general nmr behaviour of Nazirpsios can be established and that deviations from the general pattern signify differences in the material involved.

3.2.2 Nazirpsio: Phosphorous Resonance

The P^{31} resonance (gyromagnetic ratio of 17.236 MHz/tesla) was observed at 1.5 tesla but the resonance was narrower than the inhomogeneity width of the magnet. P^{31} was then studied at room temperature at 5 tesla with a superconducting magnet which had better resolution and for which the higher operating frequency gave improved signal to noise. The resonances for the CANMET samples x=1.8,1.9,2.0 (monoclinic structure) were identical and an example is shown in Figure 3.9a. This is a symmetric resonance of 0.8 gauss FWHM. The phosphorous resonances for the other CANMET samples, X=2.1,2.2,2.3 (rhombohedral structure) were also identical and an example is in Figure 3.9b. This spectrum is composed of two peaks, one 0.6 gauss FWHM and one 3.5 gauss FWHM. From these six samples, the existence of 2 peaks in the phosphorous resonance is characteristic of the rhombohedral phase of

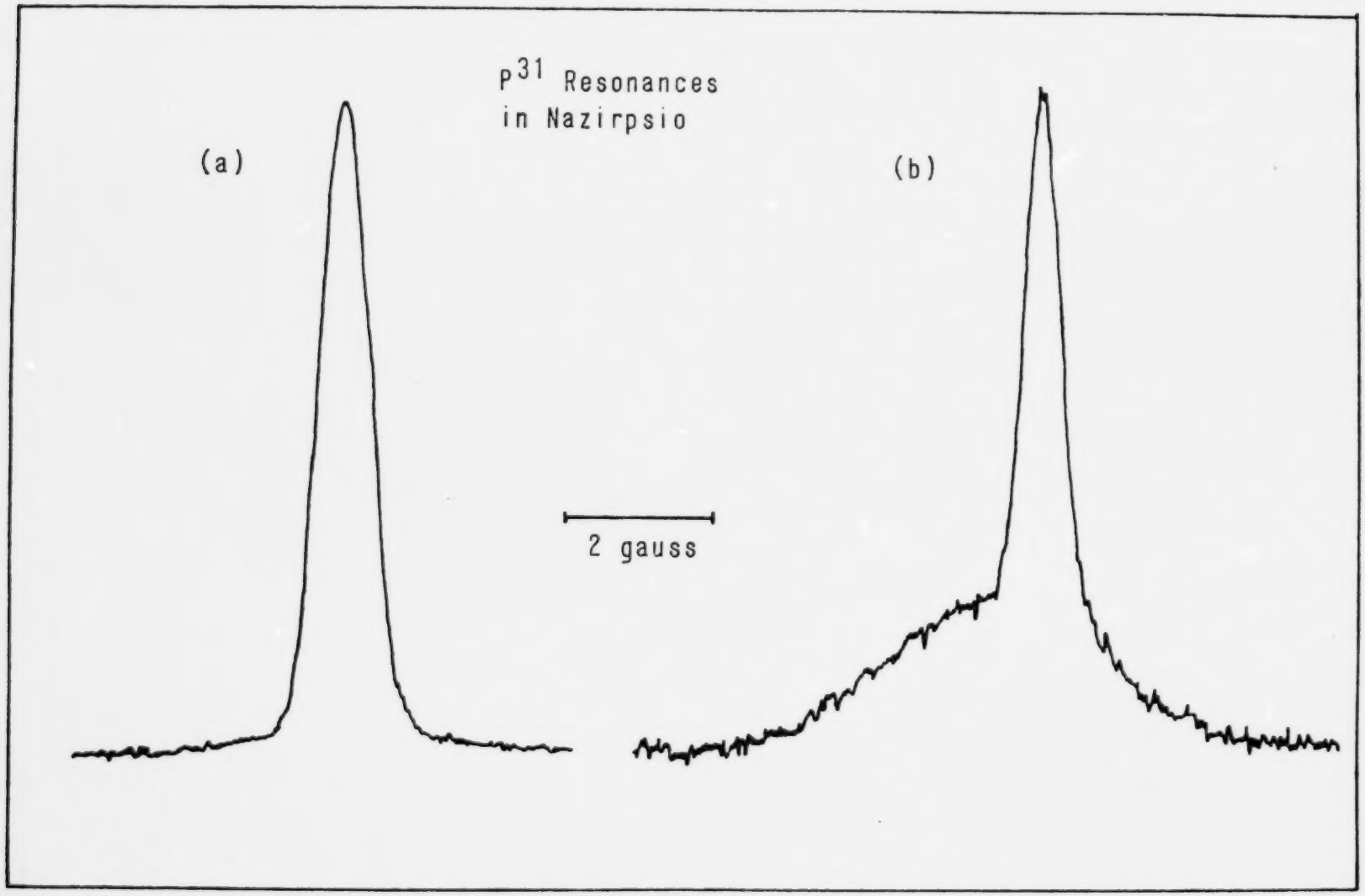

Figure 3.9
Phosphorous resonance of Nazirpsio at 5 Tesla and room temperature.
(a) resonance characteristic of monoclinic phase
(b) resonance characteristic of rhombohedral phase

Nazirpsio. The HB x=1.9 sample is monoclinic and has a phosphorous resonance the same as Figure 3.9a except for a hint of a broader component in the baseline. However, the ORF x=2.0 is the exception to the rule since its structure was monoclinic and its phosphorous resonance was similar to figure3.9b but with the broad component being about half the relative amplitude shown in this figure.

3.3 NYS

The sodium resonance of NYS at 2 tesla and room temperature is the sum of a broad resonance of 30 gauss FWHM and a narrow resonance of 5 gauss (Figure3.10). Both components of the resonance are second order quadrupole coupled. The narrow component of the resonance appears to be due to a single sodium site.

Assuming a asymmetry parameter of zero, the quadrupole coupling of the narrow component was calculated to be approximately 0.3 MHz. The lineshape of the entire sodium resonance as a function of temperature is shown in Figure 3.11. As temperature increased, the broad component began to narrow and the narrow component was no longer distinguishable. From 170 C to 250 C, the resonance does not change. At this temperature limit, the total resonance is 8 gauss FWHM and featureless. The resonance is shifted slightly to the high field side of the free ion frequency and the resonance is still second order quadrupole coupled. Because the total resonance changes shape as a function of temperature, it was not possible

Figure 3.10

Sodium resonance of NYS at room temperature and 23 MHz showing a narrow component superimposed on a broader component.

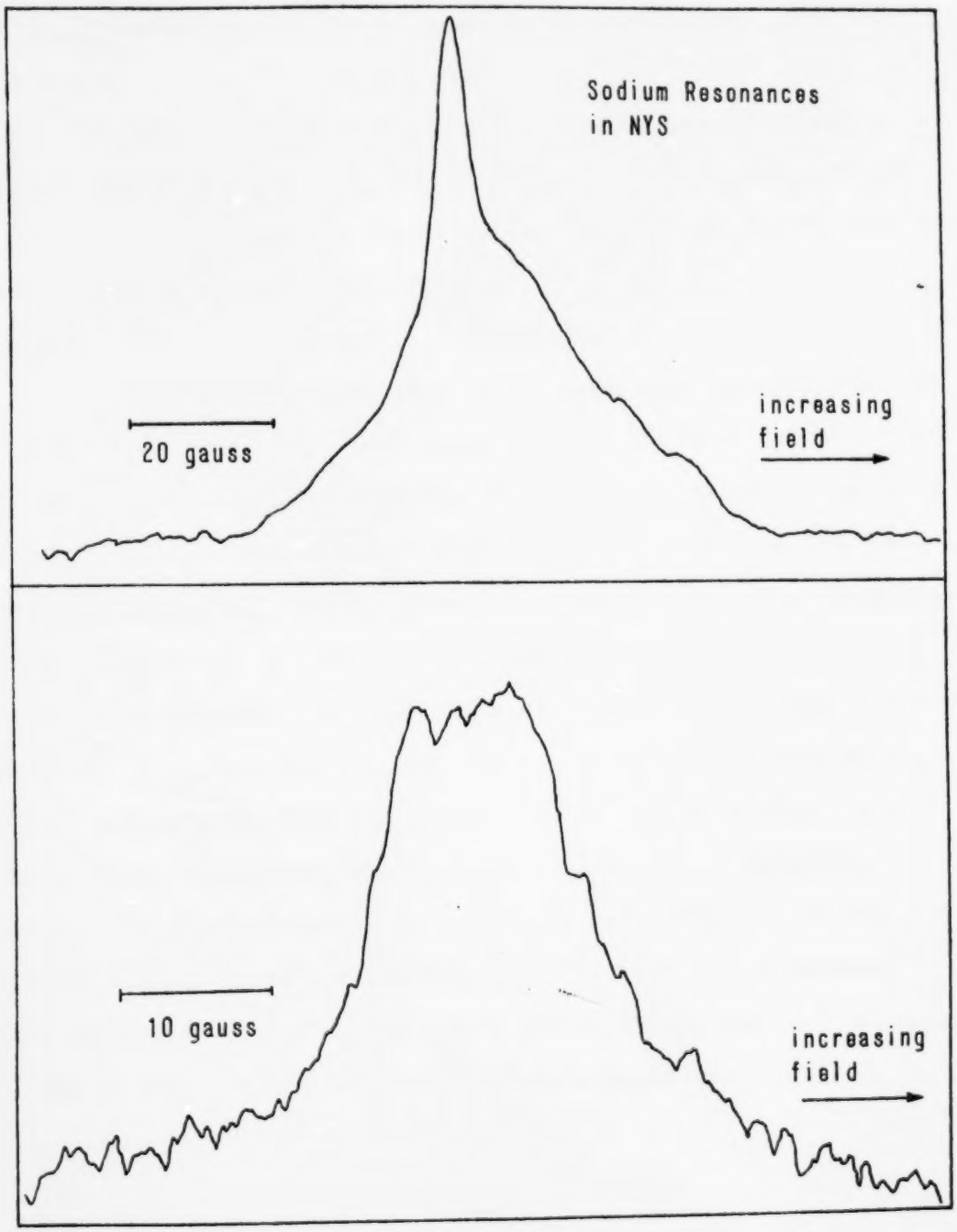

Narrow component of sodium resonance at room temperature and 6.2 MHz. The shape of the resonance is that of a single site, second order quadrupole coupled resonance.

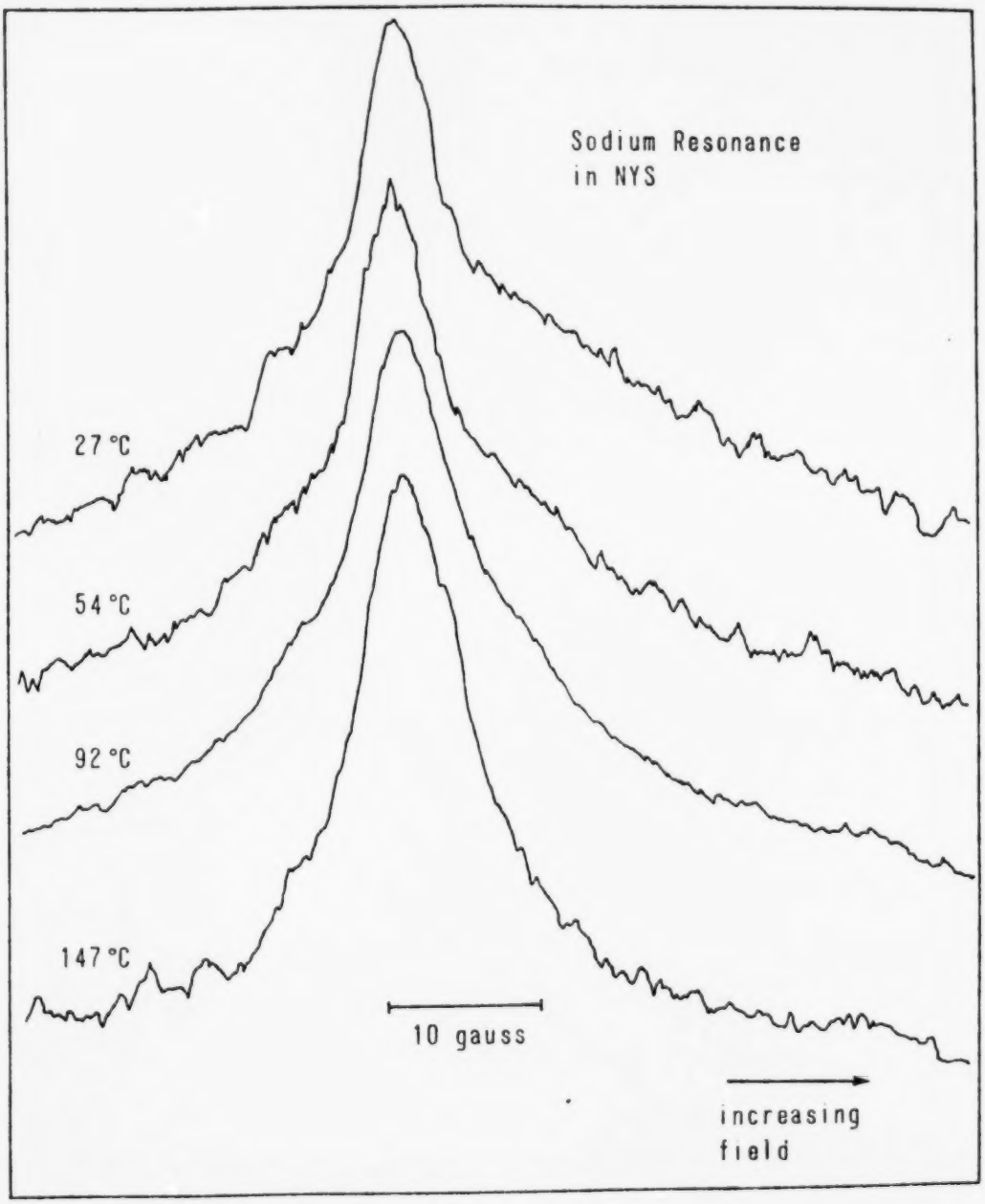

Figure 3.11

The change in the sodium resonance of NYS with temperature at 23 MHz.

to obtain quantitative information about the temperature effects. No satellite resonances were detected for the NYS samples.

The ionic conductivity of NYS was measured and gave an activation energy of 0.27+-0.02 eV and a conductivity of 0.10 $(\Omega^{-}cm)^{-1}$ at 300 C. These values are in agreement with the results of Leonova et al (1979).

3.4 NGS

The sodium resonance of NGS at room temperature and at 2 tesla is 50 gauss FWHM (Figure 3.12).Because of its width, the resonance was very difficult to observe using either slow or fast passage techniques. The resonance shape is the same as that of Nazirpsio. With increasing temperature, the resonance changes slightly to a width of 40 gauss FWHM at 250 C. Attempts to measure the resonance at fields lower than 2 tesla resulted in a very poor signal to noise ratio and the accuracy of the measurement was not enough to determine whether the resonance was second order quadrupole coupled. However, because the resonance was the same shape as Nazirpsio and shifted slightly to high field, and also since NYS showed quadrupole coupling, it was believed that the sodium resonance of NGS is also second order quadrupole coupled.

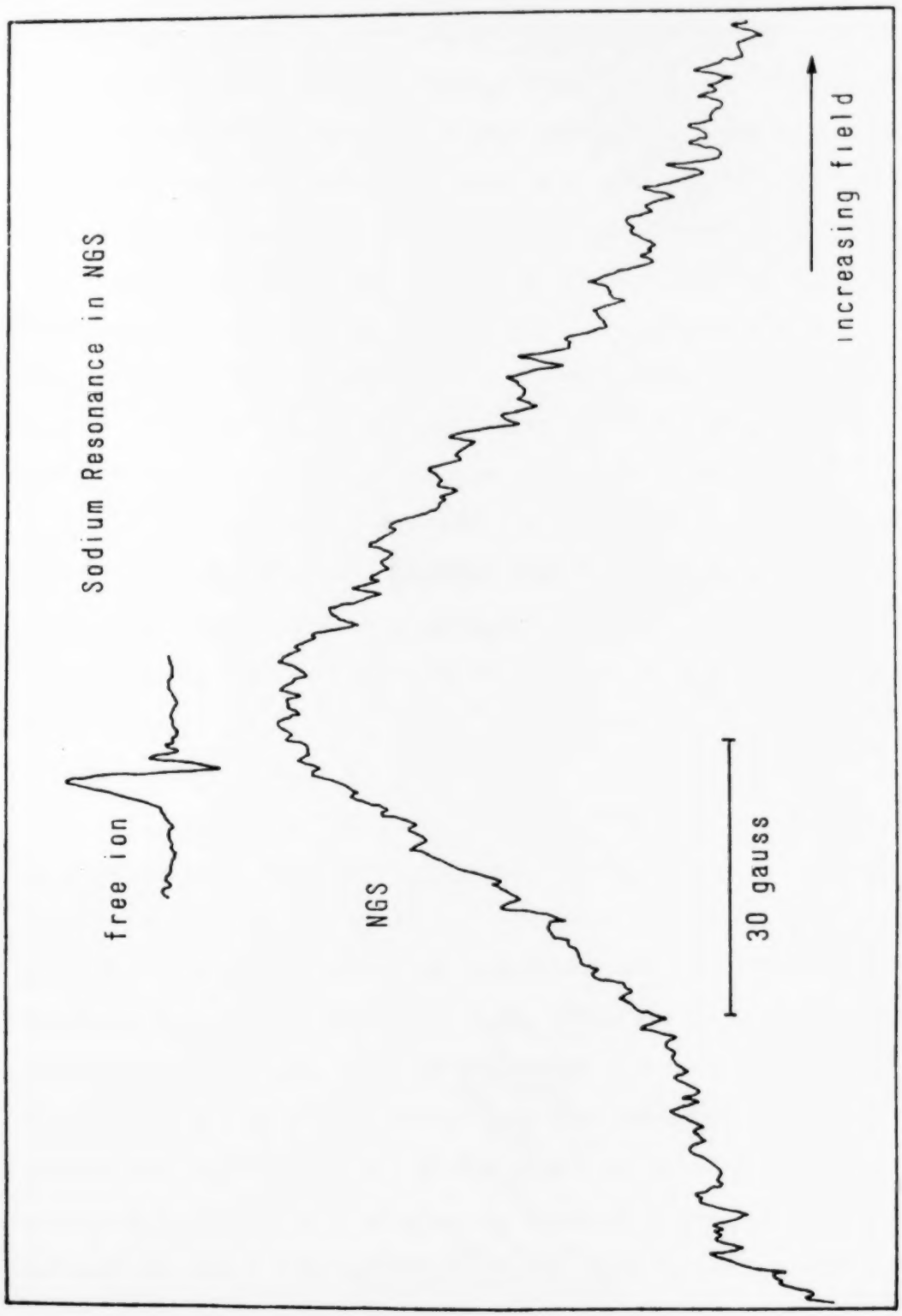

Figure 3.12 Sodium resonance of NGS at room temperature and 23 MHz.

4. DISCUSSION

Two aspects are considered in this section:

a) the use of nmr as a routine diagnostic tool for Na fast ion electrolytes

b) the specific features of nmr in the Nazirpsio system.

4.1 Diagnostics using nmr

The results show that nmr is of some use if all the resonant species is mobile. The results on NYS and NGS where a fraction of the ions are immobile show that the resonances in these cases are uninformative.

In the case of β-aluminas, it is possible to distinguish between samples from the differing shape of the resonance. However, since this is related to the $f(\beta)$ of a given sample, the relationship to conductivity is not quantitatively direct, and equivalent information is most likely obtained more directly from x-ray methods.

In the case of Nazirpsio, where the conduction is three-dimensional, all ions are mobile, and the conditions most closely approximate those of the simple isotropic theory, the nmr results are of most interest. In particular, attempt-to-escape frequencies and values of conductivity computed from the nmr data are in reasonable agreement with direct electrical properties. It is found that the nmr is capable of distinguishing deviations in properties from the norm which are reflected in electrical behaviour and it appears to be sensitive to changes in activation energy with

composition. However, the parameters of interest are derived only after a lengthy experimental procedure, and would appear to be useful principally for basic scientific studies rather than technical evaluation of materials. It may be noted that more direct information on electrical conductivity was obtained from the deviation of the radio-frequency bridge of the nmr spectrometer upon sample insertion than from the nmr. The diagnosis of the presence of protons either as part of a proton conductor or as unanticipated water of hydration or absorption is a unique feature of an nmr system.

It is likely however,that in the case of sodium ion conductors, nmr has an important role to play in understanding the properties of the materials, but the necessary investment of equipment, capital and expertise is excessive for diagnostic experiments.

4.2 Nmr in Nazirpsios

There are two very important features of the NMR of Nazirpsios that must be explained. First, why does the NMR activation energy correlate with the ionic conductivity and secondly, why does the sodium resonance become independent of magnetic field at high temperature. This has generally not been observed in previous studies of β -aluminas (Bjorkstam and Villa 1980) although in all cases of fast ion conductors the noteworthy feature in nmr is the small value of T_1 that is observed at high temperatures. In Nazirpsio the value of T_1 becomes so small that unique features have to be invoked. The

model is described in full elsewhere (Amm 1982).

It is obvious that if the resonance is not second order quadrupole coupled at high temperature that some other process must be contributing to the linewidth. The resonance at high temperature is symmetric and centered on the free ion frequency and these characteristics support the postulate that the linewidth is due to lifetime broadening. Linewidth due to lifetime broadening is the result of the Heisenberg Uncertainty Principle. That is

$$\Delta E \Delta t > h \qquad (20)$$

where ΔE is the width of an energy state and Δt is the lifetime of the state. The lifetime of the magnetic energy states is T_1, the relaxation time. If the uncertainty of the energy is written as $\Delta E = h \Delta \nu$ Then

$$\Delta \nu = 1/2\pi T_1 \qquad (21)$$

Relaxation times in Nazirpsio as short as 30 microseconds have been measured . This would give a linewidth of 5 kHz due to lifetime broadening and would thus be a significant contribution to the linewidth for the sodium resonance in Nazirpsio. Bailey et al (1976) have explained the high temperature properties of a single crystal of sodium β -Alumina in this manner.

In an attempt to explain the Nazirpsio NMR data in this work, the linewidth was assumed initially to be due to lifetime ($1/T_1$) and second order quadrupole contributions. Taking these two contributions from equations 13 and 16 and

adding them in quadrature gives the linewidth

$$(\Delta\nu)^2 = \left(\frac{1}{T_1}\right)^2 + \delta^2 \qquad (22)$$

The constants A and B in eqns.13 and 16 represent the interaction strengths of the relaxation timeand the quadrupole coupling respectively. Evaluation of the effects of different values of A/B in explaining the experimental data shown in Figure 4.1 suggests that A/B=1. In this case, at low temperatures ($\omega\tau$ large), quadrupolar effects dominate, but die away rapidly with increasing temperature, finally leaving a line width dominated by the correlation time. As noted before this is similar to the hopping frequency and would be determined by the same activation energy.

This work may be compared with other studies on sodium conducting solid electrolytes. The only other work on Nazirpsio was published by Hayes and Ailion(1979). They stated that the linewidth narrowed above 120 C at 24 MHz, as was found in this work and they went on to measure T_1 as a function of temperature. The only in depth study of the line shapes of sodium conductors as a function of temperature has been performed on sodium β-alumina. The structure of sodium β-alumina is composed of spinel blocks held apart by oxygen atoms. The sodium atoms lie in the planes between the spinel blocks and have high mobility within these planes. The sodium ion mobility parallel to the c-axis, perpendicular to the planes between the spinel blocks, is very low and the

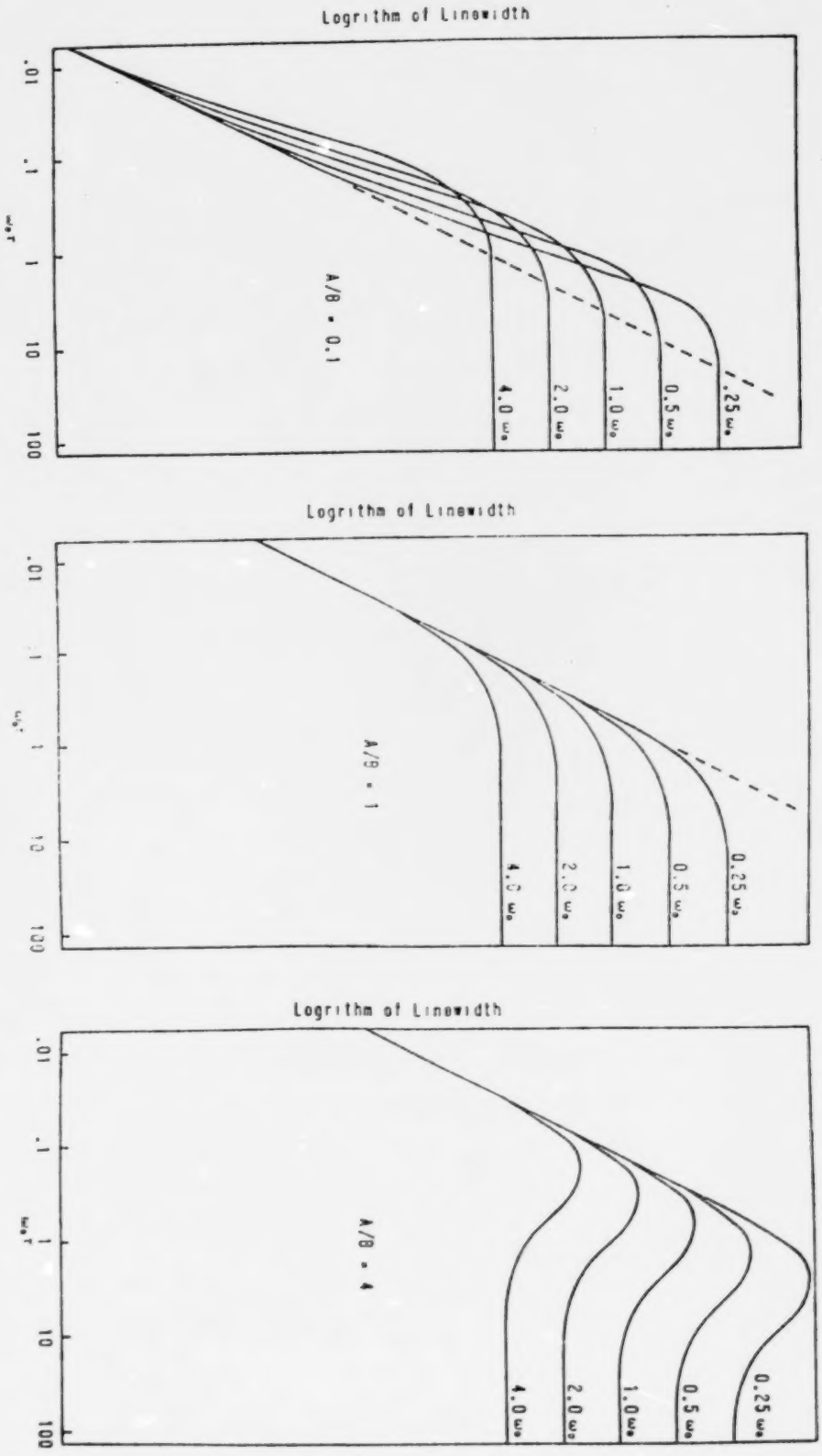

Results of a model mixing linewidths due to second order quadrupole coupling and lifetime ($1/T_1$) broadening. The constant A, is proportional to the lifetime contribution and B, is proportional to the quadrupole contribution to the linewidth.

Figure 4.1

conduction is considered to be restricted to these planes. For this reason, sodium β-Alumina is often referred to as a two-dimensional conductor. The second order quadrupole coupling in sodium β-Alumina does not decrease to a small value as a function of temperature as it does in Nazirpsio. At low temperature, the results indicate a classical second order quadrupole coupling with the maximum efg perpendicular to the c-axis (in the conducting plane). The high temperature limit is characterized similarly only with the maximum efg in the direction of the c-axis (Bjorkstam and Villa 1980). This result can be explained qualitatively by assuming the material is made up of a rigid skeleton structure and a mobile liquid-like structure. In sodium β-Alumina, the spinel blocks are the skeleton structure and the planes of sodium ions are the liquid-like structure. At low temperatures, neighbouring sodium ions in the conducting planes can give rise to an efg because of the non-isotropic distribution within the plane and also, the spinel block can give rise to an efg. At high temperatures, the conducting planes become truly liquid-like and the distribution of sodium ions around any site are isotropic within the planes. Therefore the neighbouring sodium ions cannot give rise to an efg. The efg must be due entirely to the spinel structure and the only unique direction in the spinel structure is parallel to the c-axis. This is the reason why that at high temperature, the efg is aligned with the c-axis. Because the sites that the sodium atoms hop between

are equivalent, the same efg is seen by all sodium atoms all the time and the high temperature result is classical single site, second order quadrupole coupling.

The Nazirpsios can be modelled similarly to sodium β -Alumina except that the liquid-like structure is now a three-dimensional array of sodium atoms and the sodium ions hop between three inequivalent sites. At low temperature, both the distribution of sodium ions and the rigid skeleton structure contribute to the efg. At higher temperatures, the sodium ion distribution becomes isotropic and the efg at any site is due to the rigid skeleton structure. However, because the sodium ion hops between three inequivalent sites, it sees three different efg's. Only one efg will be measured though and that will be an average of the three efg's. In the case of Nazirpsios, this average efg is almost zero or at least small enough at high temperature that the sodium resonance is no longer second order quadrupole coupled.

The sodium resonances in NYS and NGS are quite different from that of Nazirpsio because half the sodium atoms are immobile - they are part of the rigid skeleton structure. The component of the resonance from the immobile sodium ions is not expected to narrow but the efg's may change slightly at high temperature when the mobile sodium ions no longer contribute to the efg. The component of the resonance from the mobile sodium ions does not narrow either because the high temperature resonance does not contain a superimposed narrow

component. Therefore, the three mobile sites in NGS and NYS must average to a value large enough that the resonances are still second order quadrupole coupled at high temperature.

5. CONCLUSIONS

This work has undertaken a compehensive study of nmr in three types of fast ion electrolytes. It has been shown that qualitative information can be gained about most systems, but the each solid electrolyte behaves differently in NMR experiments so that the general theoretical understanding of the phenomena is not well established. However, the Nazirpsio system is usefully studied by nmr since the three-dimensional nature of the ion motion is appropriate for the application of isotropic models. A new criterion is used to measure attempt-to-escape frequencies and the factors defining the nmr linewidth are clearly established.

6. ACKNOWLEDGEMENTS

The cooperation of Dr. P.S.Nicholson in material fabrication at McMaster University is acknowledged and the assistance of CANMET staff with equipment and materials is appreciated.

REFERENCES

Abragam,A(1961) "The Principles of Nuclear Magnetism" Clarendon Press

Amm D.(1982) M.Sc thesis, Queen's University

Bailey.W,Glowinkowski.S,Story.H and Roth,W.L.(1976) J.Chem Phys. 64,4126

Bauerle.J.E (1969) J.Phys.Chem.Solids 30,2657

Bentzen.J.J and Nicholson.P.S (1980) Mat.Res.Bull. 15,1737

Bjorkstam.J.L. and Villa.M (1980) Magnetic Resonance Reviews 6,1

Bjorkstam.J.L.,Villa.M and Frye.J.S.(1981) "Nuclear and Electron Spectroscopies applied to Materials Science", E.N.Kauffman and G.K.Shenoy, Eds., 295, Elsevier,North Holland, New York

Chung.I,Story.H.S. and Roth.W.L.(1975) J.Chem.Phys. 63,4903

Hagenmuller.P and van Gool.W (1978) "Solid Electrolytes:Principles, Characterisation, Materials, Applications",Academic Press,New York

Hayes .C.E and Ailion.D.C.(1979) "Fast Ion Transport in Solids" P.Vashista,J.N.Mundy and G.K.Shenoy,eds., 297,Elesevier North Holland, New York

Kafalas.J.A. and Cava R.J.(1979)"Fast Ion Transport in Solids" Op.Cit.

Kline.D,Story.H.S. and Roth.W.L.(1972) J.Chem.Phys.57,5180

Leonova.L.S.,Tracheva.N.S.,Berestenko.V.I.,Moskvina.E.I. and Ukshe.E.A.(1979) Elektrokhimiya 15,1389

Mansingh.A,Tandon.R.P. and Vaid.J.K (1980) Phys. Rev. B21,4829

Poole.C.P.Jr. and Farach.H.A.(1972)"Theory of Magnetic Resonance" Wiley,Toronto

Richards.P.M. (1979) "Physics of Superionic Conductors" M.B.Saloman,ed.,141,Springer Verlag,New York

Segel.S.L. and Mansingh.A (1969) J.Chem.Phys.51,4578

Smith.D.S. (1982) M.Sc thesis, Queen's University

Torgeson.D.R.(1967) Rev.Sci.Instr.38,612

von Alpen.U,Bell.M.F.and Wichelhaus W.(1979) Mat. Res. Bull.14,1317

von Alpen.U,Bell,M.F. and Hofer.H.H. (1981) Solid State Ionics 3/4, 215

Wheat.T.A.,Kuriakose.A.K and Packwood R.H.(1982) Canada Centre for Mineral and Energy Technology, Energy Research Program, Mineral Sciences Laboratory, Division Report ERP/MSL 82-15(OP)

Will.F.G. (1976) J.Electrochem. Soc.123,834